博士論文

Functional Analysis of Phosphorylation Modifications within Measles Virus Nucleoprotein and Phosphoprotein

（麻疹ウイルスＮ蛋白質及びＰ蛋白質におけるリン酸化修飾の機能解析）

菅井　亮宏

CONTENTS

Functional Analysis of Phosphorylation Modifications within
Measles Virus Nucleoprotein and Phosphoprotein

GENERAL INTRODUCTION …….. 1

CHAPTER 1. Functional Analysis of the Measles Virus Phosphoprotein Phosphorylation: Regulation of viral transcriptional activity through modification at serine 86 and/or serine 151 of phosphoprotein

Introduction …… 10

Materials and Methods ……... 12

Results ……..... 15

Discussion …….. 21

Figure Legends …….. 24

Figures ……... 27

CHAPTER 2. Detailed Investigations for Phosphorylation Sites of Measles Virus Nucleoprotein: Growth kinetic analysis for recombinant viruses containing mutation in the nucleoprotein phosphorylation sites

Introduction …… 34

Materials and Methods ……... 35

Results ……..... 43

Discussion …….. 50

Figure Legends ……... 55

Figures ……..... 59

CHAPTER 3. Novelly Identified Phosphorylation Site of Measles Virus Nucleoprotein: Nucleocapsid assembly of measles virus requires a phosphorylation modification on the core domain of nucleoprotein

Introduction ……... 66

Materials and Methods …….. 68

Results ……... 75

Discussion ……. 83

Figure Legends …….. 87

Figures ……... 91

CONCLUDING REMARKS ……. 99

REFERENCES …….. 103

ACKNOWLEDGEMENT ……. 117

ABSTRACT IN JAPANESE …… 119

GENERAL INTRODUCTION

Measles virus (MV) belongs to the *morbillivirus* genus within the *Paramyxoviridae* family of the order *Mononegavirales*. The order *Mononegavirales*, possess a non-segmented negative-strand RNA genome, includes many important animal and human pathogens such as Newcastle disease virus (NDV), rabies virus, Nipah virus (NiV), Hendra virus (HeV), mumps virus, human respiratory syncytial virus, Marburg virus, and Ebola virus. Some of these viruses are causative agents of emerging or re-emerging infectious diseases, and remain serious and persistent public health threats. The *Paramyxoviridae* family includes some important zoonotic agents, for instance, NiV, HeV, and NDV. Serological surveys revealed that NiV has a wide host range including humans, pigs, dogs, cats, horses, goats, hamsters, and fruit bats (Chua, *et al*., 2003; Mohd, *et al*., 2000; Harcourt, *et al*., 2000). HeV is also emerging fatal zoonotic agent (Wang, *et al*., 2001). NDV is an economically important pathogen, causing fatal disease in many wild and domestic avian species. The *Paramyxoviridae* family also contains important animal pathogens such as rinderpest virus (RPV) and canine distemper virus (CDV), which are classified within the *Morbillivirus* genus, and thus close relatives of MV. Although animals that are susceptible to CDV infection had been thought to be the family *Canidae*, the first natural infection of CDV in a Japanese monkey (*Macaca fuscata*) was reported in 1989 (Yoshikawa, 1989). Furthermore, in 1990s, CDV infection in tigers, lions, and seals were reported one after another (Roelke-Paker *et al*., 1996; Appel *et al*., 1994; Osterhaus *et al*., 1989). Thus, several paramyxoviruses are known to infect a wide host range and sometimes cause significant cross-species transmission.

MV, the causing agent of measles, is a highly contagious human pathogen, which is characterized by fever, cough, coryza, conjunctivitis, and a maculopapular rash. MV is well known to suppress host immune responses by various mechanisms (de Vries, *et al*, 2012), and therefore measles patients often suffer from symptoms of secondary bacterial infections such as diarrhea and pneumonia. The main cause of measles deaths is typically secondary infections in respiratory and digestive tract (Shanks, *et al*., 2011; Akramuzzaman, *et al*., 2000; Beckford, *et al*., 1985). In the early 1960s, measles was a serious worldwide threat because there was no available vaccine, and it is estimated that measles caused as many as 6 million deaths per year (Hussey and Clements, 2004). However, after an attenuated measles vaccine derived from Edmonston strain was first licensed in 1963 (MacLeod, 1964), the number of measles cases reported globally has decreased dramatically. The World Health Organization (WHO) has reported that the number of estimated measles deaths during 2000 to 2011 decreased 71 percent, from 548,000 to 158,000 [Centers for Disease Control and Prevention (CDC), 2013]. Although the widespread use of effective vaccines has decreased global morbidity and mortality from measles, it remains a major cause of high mortality among children in developing countries (Bryce, *et al*., 2005; Wolfson, *et al*., 2007; CDC, 2008). CDV has almost the same historical background as MV. Live-attenuated CDV vaccines became available in the 1950s (Rockborn, 1959), which have contributed to the protection of domestic dogs against fatal infection with CDV. In recent years, however, sporadic outbreaks of CDV and MV become an issue of public health (Gemma, *et al*., 1996; Takahashi, *et al*., 2014). MV is a well-studied virus and shares many common

pathogenic features with other morbilliviruses such as CDV and RPV. Therefore findings in fundamental research of MV would be also helpful in understanding the pathological mechanism of CDV and RPV, which are one of the most important animal pathogens in the field of veterinary medicine.

MV has a non-segmented negative-stranded RNA genome containing six structural genes encoding nucleoprotein (N), phosphoprotein (P), matrix protein (M), fusion protein (F), hemagglutinin protein (H), and large protein (L) (Dowling PC, *et al*., 1986), and the P gene produces two accessory proteins, known as V and C (Cattaneo, *et al*., 1989; Bellini, *et al*., 1985). N proteins encapsidate viral genomic RNA to support viral transcription and replication by an RNA-dependent RNA polymerase L protein. The P protein is a multi-functional protein (Gely, *et al*., 2010; Sugai, *et al*., 2008; Karlin, *et al*., 2003) that assists viral transcription and replication as a cofactor of the L protein (Cevik, *et al*., 2004; Curran, 1996). The C and V accessory proteins suppress host immune responses (Ramachandran, *et al*., 2008; Shaffer, *et al*., 2003). The M protein helps virus assembly, and the F protein mediates membrane fusion, virus entry, and syncytia formation. The H protein is required for binding to the host cellular receptor (Hashiguchi, *et al*., 2011). Vaccine and laboratory-passaged strains of MV, such as Edmonston strain, has adapted to use human CD46 molecule (also known as membrane cofactor protein: this antigen is ubiquitously expressed on all nucleated cells) as a cellular receptor (Dörig, *et al*., 1994), while clinical isolates of MV cannot use CD46 (Dhiman, *et al*., 2004). Wild type MV strains are known to use SLAM (signaling lymphocyte-activation molecule: a glycoprotein expressed on activated lymphocytes

and antigen presenting cells) (Yanagi, *et al*., 2009; Dhiman, *et al*., 2004; Howie, *et al*., 2002) and nectin-4 (expressed on the basal side of polarized epithelial cells) (Pratakpiriya, *et al*., 2012; Noyce, *et al*., 2011; Mühlebach, *et al*., 2011; Reymond, *et al*., 2001). Both vaccine and clinical isolate strains infect lymphocytes and airway epithelial cells through the SLAM and nectin-4, respectively (Delpeut, *et al*., 2014; Noyce and Richardson, 2012; Tatsuo, *et al*., 2000).

N protein is the most abundant viral protein in infected cells (Ray and Fujinami, 1987), and is mainly required for viral transcription and replication. N proteins tightly associate with the viral genome and antigenome to form an N-RNA complex with a herringbone-like structure (Bhella, *et al*., 2004; Lund, *et al*., 1984). N proteins associate with every six bases of the 15,894 nucleotide viral genome and fully cover the genome RNA (Calain and Roux, 1993). This tight encapsidation allows the viral genome to be resistant to RNases and siRNAs (Bitko and Barik, 2001; Moyer, *et al*., 1990). Viral transcription and replication occur on the N-RNA complex in association with viral RNA-dependent RNA polymerase (vRdRp), composed of L and P proteins. This complex of N-RNA, P, and L is called the nucleocapsid (NC) and comprises 2,649 copies of N, about 300 copies of P, and about 20–30 copies of L (Rima and Duprex, 2009; Plumet, *et al*., 2005; Plumet, *et al*., 2005 #2). Singly-expressed N proteins associate with cellar RNA to form NC-like structures through nonspecific association (Warnes, *et al*., 1995; Fooks, *et al*., 1993; Spehner, *et al*., 1991). First, vRdRp transcribes the RNA genome and viral structural genes are expressed. When sufficient quantity of N proteins has accumulated, the function of vRdRp shifts from

transcription to replication, and the RNA genome is replicated exponentially (Plumet, *et al*., 2005). During the replication step, nascent growing viral RNA is immediately encapsidated by N protein, and vRdRp ignores gene start (GS) and gene end (GE) signals. Thus, uncapped full-length viral antigenomic RNA (positive-sense strand) is produced, which serves as a template for viral genome RNA (negative-sense strand) replication (Kolakofsky, *et al*., 2004).

MV N and P proteins have been known to be constitutively phosphorylated (Das, *et al*., 1995; Robbins, *et al*., 1980). Phosphorylation is the most general and important post-translational modification of proteins as a regulatory mechanism of the protein function. Phosphorylation modifications are deeply concerned with various intracellular events, such as protein-protein interactions, protein degradation, and cellular signal transduction, by altering protein function, conformation, and electrical charge (Sugai, *et al*., 2014; Kitchen, *et al*., 2008; Weston and Davis, 2007). Phosphorylation analyses for MV structural proteins were first reported in the late 1970s (Robbins, *et al*., 1980; Robbins and Bussell, 1979; Wechsler and Fields, 1978), and these researches demonstrated that N and P proteins of MV were phosphorylated. The phosphorylated amino acid species in the N protein were both the serine and threonine residues, while phosphorylation at only serine residue was detected within the P protein (Gombart, *et al*., 1995; Robbins, *et al*., 1980). Furthermore, during the mid-1990s, it has been also reported that some serine residues within the N-terminal half of the P protein involved in the phosphorylation reaction which was mediated by casein kinase II (Das, *et al*., 1995). Thus, phosphorylation modifications of MV

structural proteins have known for more than 40 years. However, no investigation for the functional significance of these phosphorylation modifications has been conducted until comparatively recent years.

As the name suggests, the P protein is generally phosphorylated. From researches of the P proteins in the related viruses to MV, it has been revealed that the phosphorylation of the P protein takes part in the regulation of viral gene expression. However, effect of the P protein phosphorylation has been shown to be different by each virus; CDV, RPV, and hRSV upregulated its own viral gene expression activity through phosphorylation of the P protein (Saikia, *et al*. 2008; Kaushik and Shaila, 2004; Liu, *et al*., 1997; Barik, *et al*., 1995), whereas PIV5 and BDV showed downregulation of the activity when P protein was phosphorylated (Schmid, *et al*., 2010; Sun, *et al.*, 2009; Timani, *et al*., 2008). In the case of MV, it has not been clarified whether the phosphorylation of P protein is involved in the viral transcription and replication, as with other related viruses. Additionally, there is no investigation on relationship between phosphorylation of N and P protein.

In our previous research, it has been demonstrated that phosphorylation sites of the MV N protein were the serine residues at location 479 and 510 by mass spectrometry, and the phosphorylation was involved in the regulation of transcription and/or replication in the context of minigenome assay (Hagiwara, *et al*., 2008). These serine residues at location 479 and 510 are conserved among almost all of MV strain, suggesting that these phosphorylation sites are biologically significant during the viral life cycle.

Hence, in this study, to clarify the functional significance of the phosphorylation of MV N and P protein, the author conducted detailed investigation of the N and P protein phosphorylation.

CHAPTER 1

Functional Analysis of the Measles virus phosphoprotein phosphorylation:

Regulation of viral transcriptional activity through modification at

serine 86 and/or serine 151 of phosphoprotein

CHAPTER 1

INTRODUCTION

In CHAPTER 1, the author examined the phosphorylation status of MV N and P protein during transcription and replication, and reported the relevance of the N and P protein phosphorylation to viral gene expression.

MV P protein is a cofactor of the viral RNA polymerase (L protein) that associates with the nucleoprotein-RNA complex to support viral transcription and replication (Rima and Duprex, 2009). In *Mononegavirales*, P protein undergoes phosphorylation (Das, *et al*., 1995; Robbins, *et al*., 1980; Robbins and Bussell, 1979; Wechsler and Fields, 1978), and many recent reports have highlighted a relationship between phosphorylation of P protein and viral gene expression (Sun, *et al*., 2009; Saikia, *et al*., 2008; Schmid, *et al*., 2007; Kaushik and Shaila, 2004; Huntley, *et al*., 1997; Liu, *et al*., 1997; Barik, *et al*., 1995; De, *et al*., 1995; Gao and Lenard, 1995; Huntley, *et al*., 1995). N protein is also known to be phosphorylated (Gombart, *et al*., 1995; Robbins, *et al*., 1980; Robbins and Bussell, 1979; Wechsler and Fields, 1978). Our recent research identified the major phosphorylation sites of MV N protein at S479 and S510 (Hagiwara, *et al*., 2008). Alanine-substitution of these phosphorylation sites of N protein caused decrease in viral gene expression at virus minigenome experiment, suggesting that phosphorylation of N protein takes part in the viral transcription and/or replication. Thus, phosphorylation of both N and P proteins are thought to be important for viral gene expression. But detail of relationship between N protein phosphorylation and viral RNA transcription/replication is not clarified, and there was no research

demonstrating relevance between phosphorylation of P protein and viral transcription/replication activity in MV.

To further elucidate the mechanism of viral gene transcription and replication, clarification of the roles of N and P protein phosphorylation are needed. In present study, the author focused on the relationship between viral transcription/replication activity and phosphorylation of P protein, because our resent study suggested mutation of N phosphorylation sites raises P protein phosphorylation, and statistically significant inverse correlation has found between P phosphorylation and viral gene expression activity. Here, the author reports that N protein phosphorylation could influence the phosphorylation status of P protein, and the phosphorylation of P protein is involved in regulation of viral transcription through changes in its phosphorylation status.

CHAPTER 1

MATERIALS AND METHODS

Cells and antibodies

HEK (human embryonic kidney) 293 and COS-7 (SV40 transformed African green monkey kidney fibroblast) cells (Gluzman, 1981) were propagated in Dulbecco's modified Eagle's medium (Sigma) supplemented with 5% fetal bovine serum (JRH Bioscience), 2 mM L-glutamine, 100 U/ml penicillin, and 0.1mg/ml streptomycin at 37ºC in 5% CO_2. Anti-MV N polyclonal antibody was prepared as described previously (Hagiwara, *et al*., 2008).

Plasmids

The construction of the pCAGGS mammalian expression vectors (Niwa, *et al*., 1991) containing N, N mutants (S479A, E480A, G509A, S510A, D511A, and S479A/S510A), P, P mutants (S86A/S151A and T49A/S86A/S151A), and L genes from MV-HL strain (Kobune, *et al*., 1996) was as described (Hagiwara, *et al*., 2008). In this study, the expression plasmid of P protein was modified to not express C protein, which is an accessory protein encoded in the P protein gene.

In vitro transcription of minigenomic RNA

pMDB1 vector (Baron and Barrett, 1997) containing the firefly luciferase gene possessing the leader and trailer sequence of the MV-HL strain (1-107 leader and 15786-15894 trailer nucleotides) (Hagiwara, *et al*., 2008) was used for *in vitro*

transcription with RiboMAx Large Scale RNA Production System (Promega) according to the manufacturer's instructions. RNA products were purified using MicroSpin G25 columns (Amersham Biosciences) followed by phenol-chloroform extraction. Purified minigenomic RNA was concentrated by 2-propanol precipitation and was dissolved into small amount of water.

Minigenome assay

Precise methods for the minigenome assay have been described previously (Hagiwara, *et al*., 2008). Briefly, 293 cells in 24-well plates were transfected with N-, P-, and L-protein expression plasmids using Lipofectamine LTX Reagent (Invitrogen) and Plus Reagent (Invitrogen), and viral minigenomic RNAs encoding firefly luciferase were transfected with Lipofectamine 2000 Reagent (Invitrogen) the following day. After 24 h, cells were lysed in Passive Lysis Buffer (Promega), and luciferase activity was measured using a PicaGene Luminescent Kit (Tokyo Ink Manufacturing) according to the manufacturer's instructions. Fluorescent intensity was detected by a luminometer Mini Lumat LB 9506 (Berthold).

Immunoprecipitation

COS-7 cells (5×10^5) were transfected with N and P plasmid, and 293 cells (5×10^5) were transfected with plasmids for N, P, L, and minigenomic RNA for firefly luciferase using the method described above. At 24 h post transfection, 0.38 mCi/ml of ^{32}P (phosphorus-32 Radionuclide, PerkinElmer) or 0.06 mCi/ml of ^{35}S (EasyTag EXPRESS

Protein Labeling Mix, PerkinElmer) was added to the media, and incubation continued at 37°C for 24 h. Cells were harvested and lysed in lysis buffer (0.5mM of EDTA and 0.5% of TritonX-100 in PBS) supplemented with Protease Inhibitor Cocktail (BD Biosciences) and PhosSTOP Phosphatase Inhibitor Cocktail (Roche) for 1 h at 4°C, and cell debris was removed by centrifugation. After preclearing the lysate with Protein A Sepharose CL-4B (Amersham Biosciences) beads, lysates were incubated with protein-A beads and anti-MV N polyclonal antibodies for 16 h at 4°C. Beads were collected and washed five times with PBS, and suspended in 2x Laemmli's SDS sample buffer. Component proteins were separated by SDS-PAGE and radioactivity detected using phosphorimager FLA-5100 (Fujifilm). Quantitative analyses of bands was performed three times and quantified by Image Gauge (Fujifilm).

Quantitative RT-PCR

293 cells were transfected with plasmids for N, P, L, and minigenome RNA by the method described above. Total RNAs were extracted from the cells using ISOGEN (NipponGene). Minigenome RNA, Fluc mRNA, and GAPDH mRNA levels in the total RNAs were quantified by real-time RT-PCR using PrimeScript Reverse Transcriptase (Takara), SYBR Premix Ex Taq (Takara) and Rotor-Gene Q (QIAGEN).

RESULTS

1.1. Inverse relationship between phosphorylation intensity of P protein and viral gene expression activity

Our previous study demonstrated that alanine substitution at major phosphorylation sites of MV-N protein (S479A, S510A, and double mutant S479A/S510A) downregulates viral transcription and/or replication in a minigenome assay (Hagiwara, *et al*., 2008). This assay is a widely used method for measuring the RNA polymerase activity of the viral transcription/replication complex (N, P, and L proteins associated with minigenomic RNA) via expression of a reporter gene with the leader and trailer untranslated regions of viral genomic RNA (Baron and Barrett, 1997; Brown, *et al*., 2005). In the previous research, wild type (wt) N, S479A, and S510A proteins expressed alone in cultured cells were strongly labeled with ^{32}P, whereas the S479A/S510A mutant showed significant reduction in phosphorylation level (Hagiwara, *et al*., 2008). The author used the same method to detect the phosphorylation status of N protein during transcription/replication by investigating the phosphorylation level of N protein in presence of P, L, and minigenomic RNA. The phosphorylation pattern of N protein in the assay was different from when N protein was expressed alone. The phosphorylation level of S479A was markedly higher than wt or another N protein mutant. S479A/S510A showed a very low level of phosphorylation and wt-N and S510A showed a moderate level (Fig. 1A and 1B). However, no significant correlation

was found between N protein phosphorylation level and transcription/replication activity, under any conditions (Fig. 1E). Interestingly, however, immunoprecipitation (IP) demonstrated that the presence of N protein mutants changed the phosphorylation status of P protein. P protein that was coprecipitated with wt-N protein showed a low phosphorylation level, while P protein coprecipitated with N protein mutants (S479A, S510A, and S479A/S510A) was highly phosphorylated (Fig. 1C and 1D). Of note, highly phosphorylated P protein corresponded well with abrogation of viral RNA expression, and the phosphorylation level of P protein was inversely related to transcription/replication activity in the minigenome assay (Fig. 1D and 1E). Taken together, these results implied that changes in the phosphorylation status of N protein indirectly downregulate the reporter gene expression through altering phosphorylation intensity of P protein.

1.2. P protein Phosphorylation is affected by phosphorylation status of N protein

Alanine substitution at major phosphorylation sites of N protein (S479A, S510A, and S479A/S510A) promoted P protein phosphorylation via N-P protein interaction. To determine whether elevation of P protein phosphorylation was caused by changes in the phosphorylation status of N protein or were independent of N protein phosphorylation, the author generated additional N protein mutants with alanine substitutions at amino acids adjacent to major phosphorylation sites (E480A, G509A, and D511A). The author used IP to examine the phosphorylation level of the P protein

associated with these N protein mutants. The S479A, S510A, and S479A/S510A mutants of N protein increased P protein phosphorylation, while E480A, G509A, and D511A mutants of N protein caused no change in the phosphorylation status of P protein (Fig. 2A and 2B). Thus, the increase in P protein phosphorylation was accompanied by changes in N protein phosphorylation status. These data suggested that both S479 and S510 of N protein must be phosphorylated to maintain P protein at its basal phosphorylation level, and the absence of a phosphate group at S479 and/or S510 caused enhancement of P protein phosphorylation and downregulation of viral transcription/replication. In other words, phosphorylation of P protein that caused downregulation of viral transcription/replication could be induced by modulation of N protein phosphorylation.

1.3. Phosphorylation at S86 and/or S151 of P protein is critical for downregulation of viral transcription/replication

S86 and S151 of MV-P protein are reported to be sites for phosphorylation by casein kinase II (CKII) (Das, *et al*., 1995). T49 of MV-P protein is homologous to the major phosphorylation site of rinderpest virus (RPV) P protein, which is a closely related morbillivirus (Saikia, *et al*., 2008; Kaushik and Shaila, 2004). To further clarify the correlation between phosphorylation of P protein and viral transcription/replication activity, the author generated mutants of P protein whose phosphorylation sites were substituted with alanine residues: S86A/S151A (dP) and T49A/S86A/S151A (tP). IP

and minigenome assay were conducted using mutants of N and P protein. IP results demonstrated that the phosphorylation levels of dP and tP did not significantly decrease compared to wt-P protein associated with wt-N protein (Fig. 3A and 3B). This indicated that the substituted sites of dP and tP were not constitutively phosphorylated. In contrast to wt-P protein, the phosphorylation levels of dP and tP were not enhanced by association with N protein mutants (S479A, S510A, and S479A/S510A) (Fig. 3A and 3B). This suggested that the elevation in the phosphorylation of P protein was due to phosphorylation at S86 and/or S151. Furthermore, comparison of dP and tP showed that alanine substitution of T49 did not decrease phosphorylation of P protein. Therefore, T49 was not important as a phosphate group acceptor.

By minigenome assay, the alanine substitutions in the dP and tP mutants did not impair the function of P protein as a cofactor of RNA polymerase (Fig. 4A). N protein with mutations at major phosphorylation sites downregulated transcription/replication in association with wt-P protein, but failed to decrease transcription/replication activity in combination with dP or tP (Fig. 4B-D). Hence phosphorylation at S86 and/or S151 of P protein was likely to play an important role in downregulation of viral transcription/replication. Additionally, since mutations of dP (S86 and S151) were sufficient to restore the decreased transcription/replication activity, the T49 site of P protein was not necessary for regulation of transcription/replication in MV (Fig. 4B-D). Collectively, downregulation of viral transcription/replication in the minigenome assay was caused by an elevation in the phosphorylation level of P protein, specifically at S86 and/or S151.

1.4. Statistical evaluation of correlation between P protein phosphorylation intensity and viral transcription/replication activity

To calculate the correlation between the phosphorylation level of MV P protein and viral transcription/replication activity, the author quantified the intensity of phosphorylation by densitometry. Its correlation with viral transcription/replication activity was represented as a coefficient of determination (r^2). On scatter diagrams, a strong inverse correlation was observed between the phosphorylation level of P protein and viral transcription/replication activity, implying that viral transcription/replication was affected by the total phosphorylation level of P protein. Furthermore, the best-fit curve of the relationship was obtained by exponential approximation ($r^2 = 0.97$) (Fig. 5A) rather than linear approximation ($r^2 = 0.78$) (Fig. 5B), and an acquired regression curve suggested that transcription/replication activity was abruptly attenuated when P protein exceeded an optimum phosphorylation level. Therefore, strong phosphorylations at 86S and 151S sites were likely to be important for negative regulation of transcription/replication. In contrast, N protein phosphorylation intensity had no correlation with viral transcription/replication, with a coefficient of determination of 0.0018 (Fig. 5C).

1.5. Phosphorylation of P protein at S86 and S151 selectively downregulated viral transcriptional activity

To determine which step in viral RNA synthesis was affected by P-phosphorylation, the author measured viral transcription and replication efficiency by quantitative RT-PCR under the same condition as minigenome assay. As a result, transcription efficiency (mRNA/minigenome) of mutants of N protein (S479A, S510A, and S479A/S510A) was significantly reduced from 27.9 to 33.1%, while replication efficiency (minigenome) showed no significant differences (Fig. 6A and 6C). Quantities of Fluc mRNA corresponded with the pattern of Fluc activity in minigenome assay (Fig. 1E and 6B). These data suggest that downregulation of viral RNA synthesis accompanied with P-phosphorylation at S86 and S151 was caused by decrease in transcriptional activity rather than replication. Slight differences in replication efficiency were not correlated with phosphorylation level of P protein; therefore these differences in replication may not be caused by P phosphorylation.

DISCUSSION

The author found that N protein and the mutants S479A, S510A, and S479A/S510A showed a different phosphorylation pattern during viral transcription/replication than N protein expressed alone in cultured cells. Since N protein coimmunoprecipitated with P protein showed different phosphorylation pattern, N-P protein association could change the phosphorylation status of N protein. Additionally, N-P association also affected the phosphorylation status of P protein. It was revealed that phosphorylation of N protein was indirectly involved in the efficiency of viral RNA synthesis in the minigenome assay. As shown in Figure 5 and 6, a strong inverse correlation was found between the phosphorylation level of P protein and viral transcriptional activity. Phosphorylation of P protein has generally believed to be connected with upregulation in viral RNA synthesis. For instance, removal or inhibition of kinase activity for P protein decreases transcription/replication activity or viral growth in canine distemper virus (Liu, *et al*., 1997), sendai virus (Huntley, *et al*., 1997), human parainfluenza virus type 3 (De, *et al*., 1995; Huntley, *et al*., 1995), and vesicular stomatitis virus (Gao and Lenard, 1995). As a more direct approach, site-directed mutagenesis at the phosphorylation site of P protein causes a decrease in viral gene expression in rinderpest virus (Saikia, *et al*., 2008; Kaushik and Shaila, 2004) and human respiratory syncytial virus (Barik, *et al*., 1995). These phosphorylation sites seem to be required for efficient P protein function. Recently, however, mutation at the phosphorylation sites of P protein increased viral gene expression activity in parainfluenza type 5 (PIV5) (S308) (Sun, *et al*., 2009;

Timani, *et al*., 2008) and borna disease virus (BDV) (S26, S28) (Schmid, *et al*., 2007; Schmid, *et al*., 2010). In PIV5, increased viral gene expression causes induction of cell death and expression of cytokines such as IFN-β and IL-6. Viral gene expression of PIV5 is negatively regulated by phosphorylation of P protein, enabling efficient avoidance of host immune responses (Sun, *et al*., 2009). In BDV, negative regulation by phosphorylation of P protein has been suggested as a prerequisite for efficient viral dissemination (Schmid, *et al*., 2010). As a common mechanism among *Mononegavirales*, in addition to constitutive phosphorylation sites that are necessary for activity, MV-P protein could also possess regulatory phosphorylation sites to maintain a transcription level. If MV uses the same strategy as PIV5 and BDV, S86 and S151 would be strong candidates for regulatory phosphorylation sites in MV-P, and phosphorylation of P protein at S86 and/or S151 could serve as negative regulator of viral gene expression for efficient viral growth.

Although the major phosphorylation sites S479 and S510 of N protein are adjacent to the binding region for P protein (Bernard, *et al*., 2009; Houben, *et al*., 2007; Longhi, *et al*., 2003), mutations caused no impairment in N-P association by IP (Fig. 1A and 1C) or complex formation assay (Hagiwara, *et al*., 2008). Of note, the double mutant (S479A/S510A) showed higher activity than either single mutant (S479A, S510A) in a minigenome assay (Fig.1E). Furthermore, mutations at contiguous sites of N protein phosphorylation sites failed to enhance P protein phosphorylation (Fig. 2). These findings suggest that excessive phosphorylation of P protein caused by N protein mutants is probably not responsible for a structural abnormality of N protein, but relies

on a change in its phosphorylation properties. The findings in this chapter could provide a new regulatory mechanism of viral gene expression: phosphorylation at S86 and S151 of MV-P protein is generally suppressed, and change in the phosphorylation status of N protein or direct phosphorylation at S86 and S151 of the P protein, resulting in reduction of viral gene expression. Hence, a dephosphorylation system for N protein might serve as a switch for P protein activity.

Phosphorylation status of measles virus N protein has been investigated under various conditions since the late 1970s. Some papers reported that no difference was found between phosphorylation status of N protein from nucleocapsids or virions in acutely infected cells and persistently infected cells (Robbins, *et al*., 1980; Robbins and Bussell, 1979). It was also reported that free N protein and nucleocapsid-associated N protein showed different phosphorylation pattern (Gombart, *et al*., 1995; Kawai, *et al*., 1999). However influence of N-P interaction on its own phosphorylation status has not been studied. In this report, the author demonstrated that N and P protein changes own phosphorylation status through N-P interaction. Thus, the presence of P protein is important when considering the changes of N-phosphorylation status, and this finding would help the understanding of the past reports of N-phosphorylation. Biological significance of the changes in phosphorylation status of N and P protein through the viral life cycle is unknown. However, downregulation of transcription via phosphorylation at S86 and/or S151 of P protein could be a key step in determining the role of N and P protein phosphorylation.

FIGURE LEGENDS

Fig. 1

Correlation between phosphorylation level of P protein and transcription/replication activity. 293 cells were transfected with expression plasmids for N, P, L, and minigenome RNA, and lysates used for IP and minigenome assay. (A) ^{32}P or ^{35}S-labeled N proteins were immunoprecipitated with anti-N protein polyclonal antibodies and separated by SDS-PAGE. (B) Phosphorylation levels of N protein were quantified by densitometry. (C) ^{32}P or ^{35}S-labeled P protein coprecipitated with N protein was detected the same time with N protein. (D) Phosphorylation levels of P protein were quantifed. (E) Minigenome assay using a series of N protein mutants. * $p < 0.05$, ** $p < 0.01$. Error bars indicate standard deviations.

Fig. 2

N protein mutants with alanine substitutions at residues adjacent to major phosphorylation sites do not enhance phosphorylation of P protein. (A) P protein expressed in COS-7 cells with various N protein mutants (without L protein and minigneome RNA), and IP was performed with anti-N polyclonal antibody. (B) Densitometry of the bands of P protein coprecipitated with N protein mutants.

Fig. 3

Phosphorylation levels of dP and tP were not enhanced by association with N protein

mutants. (A) Various pair of RI labeled-N and -P protein mutants expressed in 293 cells under presence of L protein and minigenome RNA were immunoprecipitated using anti-N polyclonal antibody. dP: S86A/S151A, tP: T49A/S86A/S151A. The graphs show the densitometry of (B) N and (C) P protein bands. ** $p < 0.01$

Fig. 4

Transcription/replication activity was affected by phosphorylation status of P protein rather than N protein. Wt-P, dP (S86A/S151A), and tP (T49A/ S86A/S151A) were subjected to minigenome assay in pairs with (A) wt-N, (B) N (S479A), (C) N (S510A), and (D) N (S479/510A). * $p < 0.05$, ** $p < 0.01$, *** $p < 0.001$. Error bars indicate standard deviations.

Fig. 5

Viral transcription/replication activity was inversely related to the total phosphorylation level of P protein in exponential manner. From Figures 3 and 4, relationships between the phosphorylation level of P protein and viral transcription/replication activity for various pairs of mutants were plotted on scatter diagrams, and significant correlations found. Correlation was represented by (A) exponential approximation ($r^2 = 0.97$) rather than (B) linear approximation ($r^2 = 0.78$). (C) Phosphorylation of N protein had no correlation with transcription/replication ($r^2 = 0.0018$).

Fig. 6

Quantitative RT-PCR of minigenome RNAs and its transcripts. Minigenome RNAs and its transcripts were detected by quantitative RT-PCR from 293 cells that transfected with plasmid for N (wt, S479A, S510A, and S479A/S510A), P, L, and minigenome RNA by the same method of minigenome assay. Reverse transcription was performed with oligo-dT or minigenome specific primer (GGCCGTCATGGTGGCGAATACCAA ACAAAGTTGGGTAAGGATAGATCAATCAATGATC), and following real-time PCR was performed with primer pairs for the minigenome (F: GGCCGTCATGGTGGCGAAT/R: AGCGTAAGTGATGTCCAC), the transcripts (F: GTACACGTTCGTCACATCTC/R: CGCAGGCAGTTCTATGAGGC), and GAPDH (F: AACATCATCCCTGCCTCTACTG/R: GCTTCACCACCTTCTTGATGTC). (A) minigenome RNA levels (B) Fluc mRNA levels (C) transcription efficiency. * $p < 0.05$. Error bars indicate standard deviations.

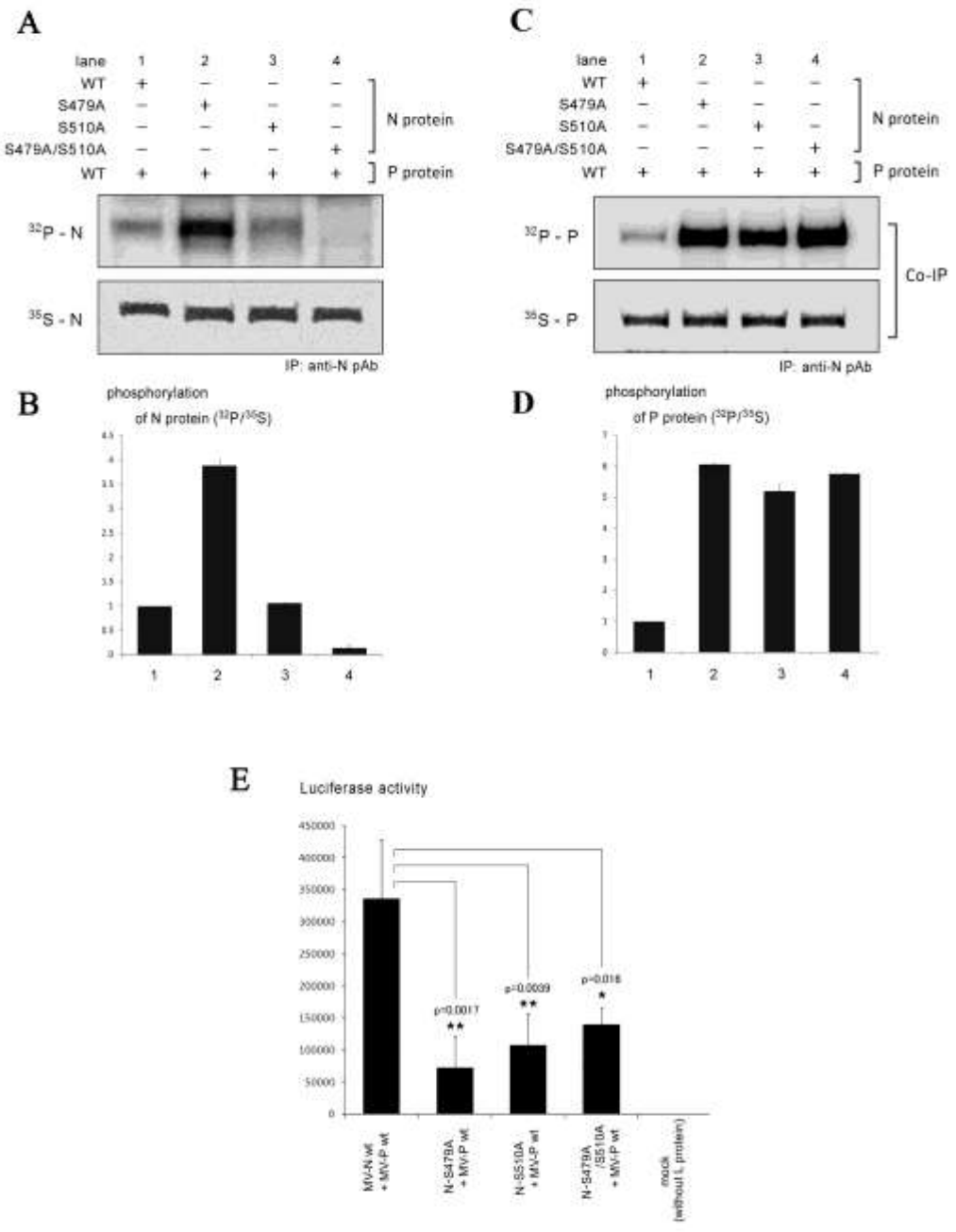

Chapter 1 - Figure 1

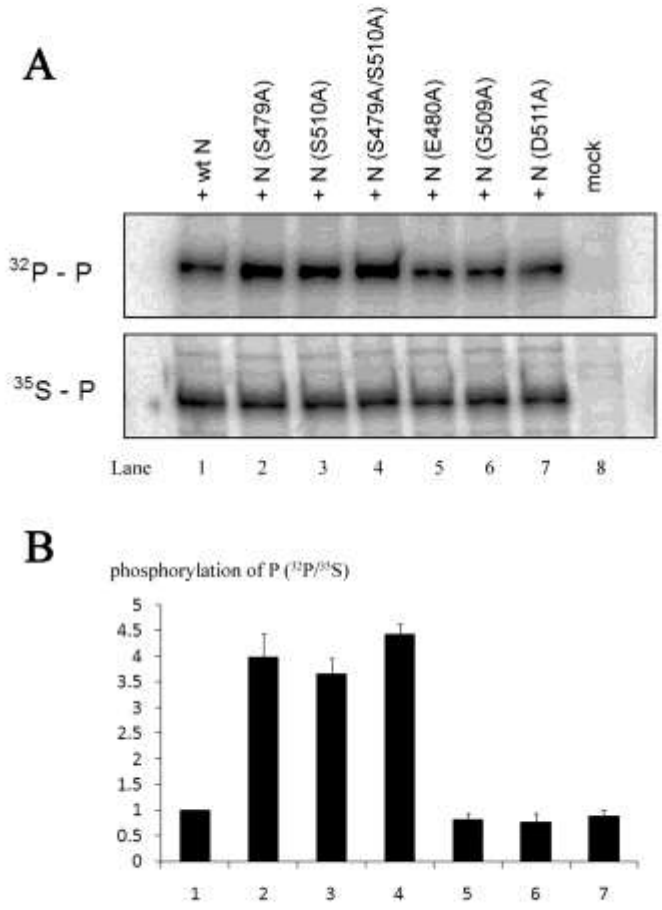

Chapter 1 - Figure 2

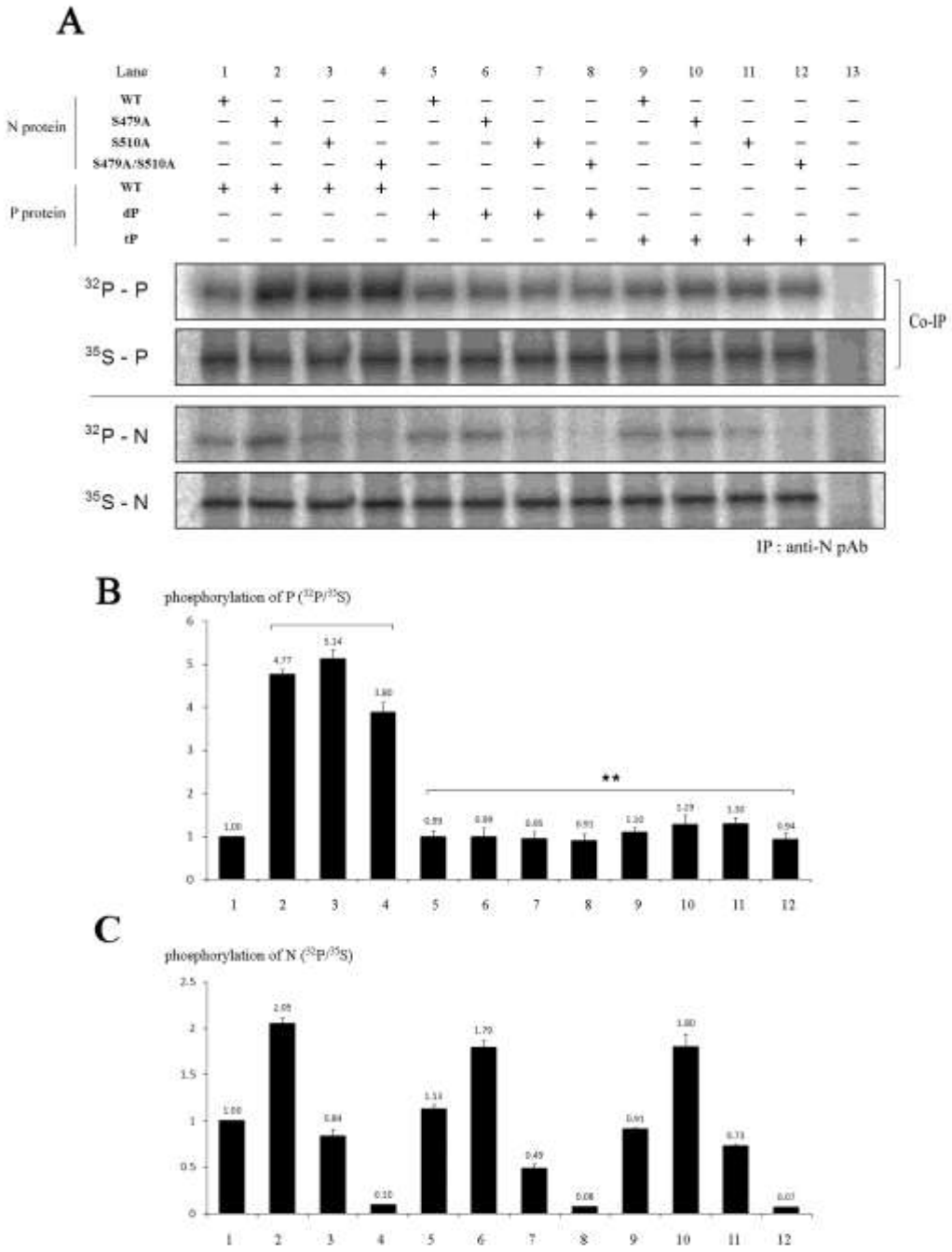

Chapter 1 - Figure 3

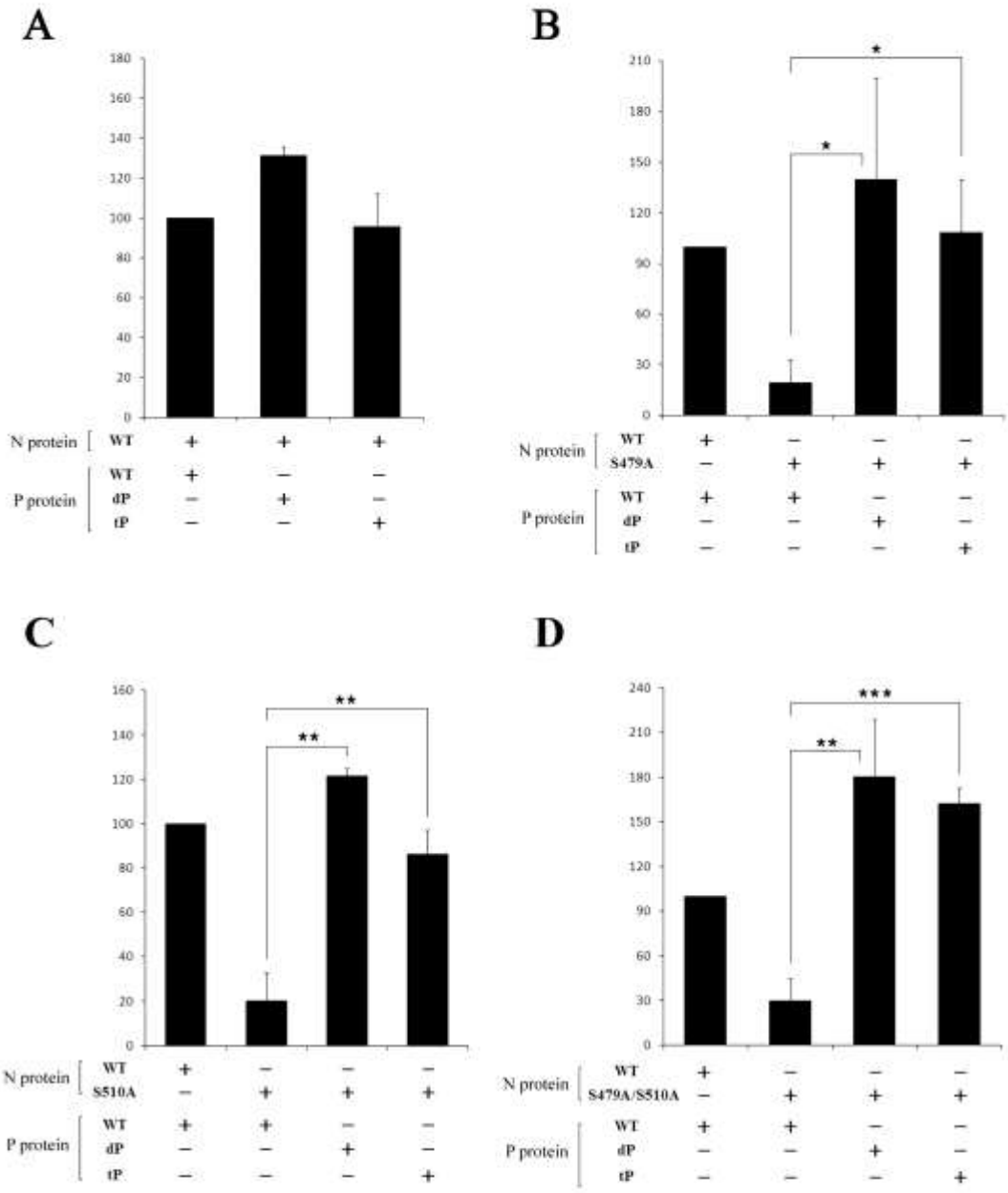

Chapter 1 - Figure 4

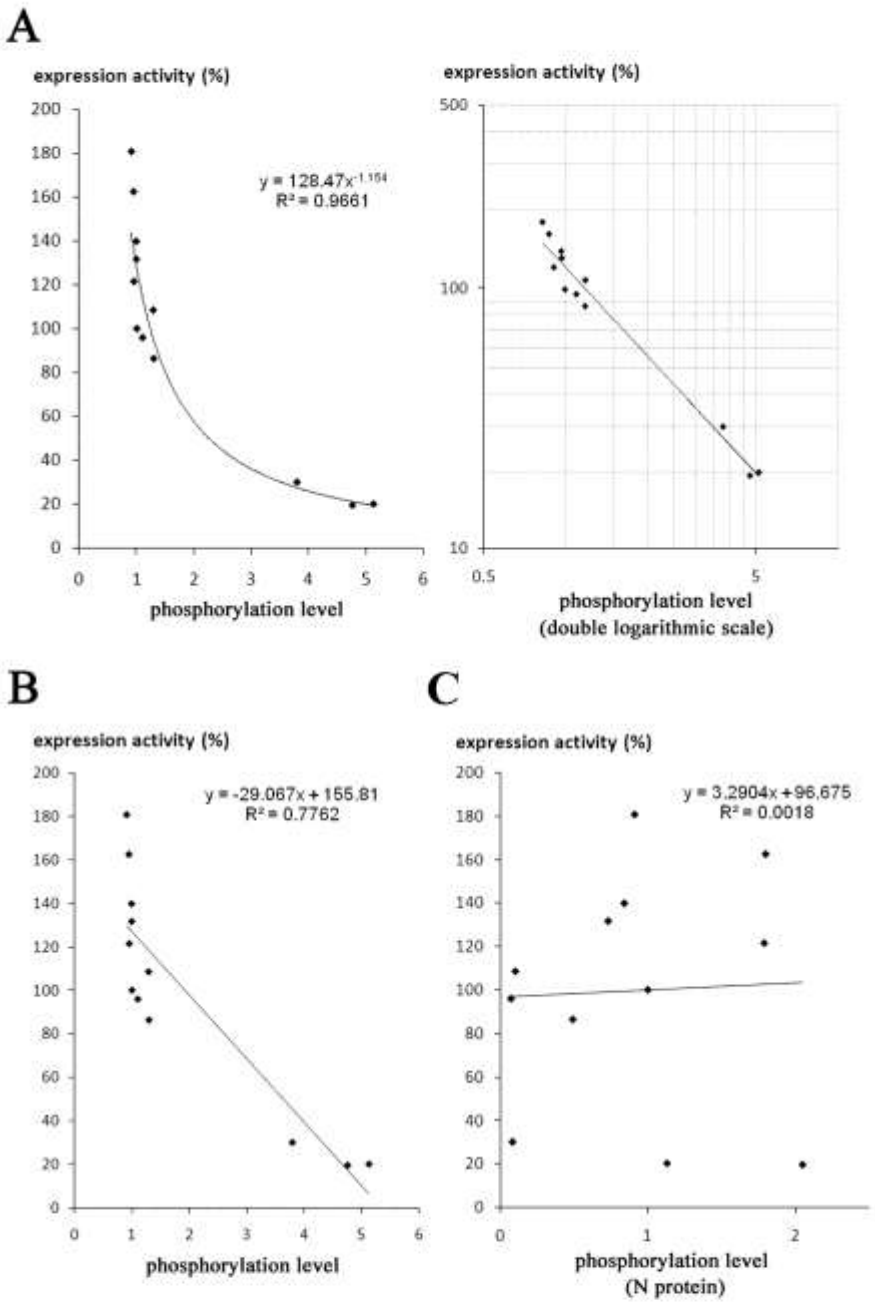

Chapter 1 - Figure 5

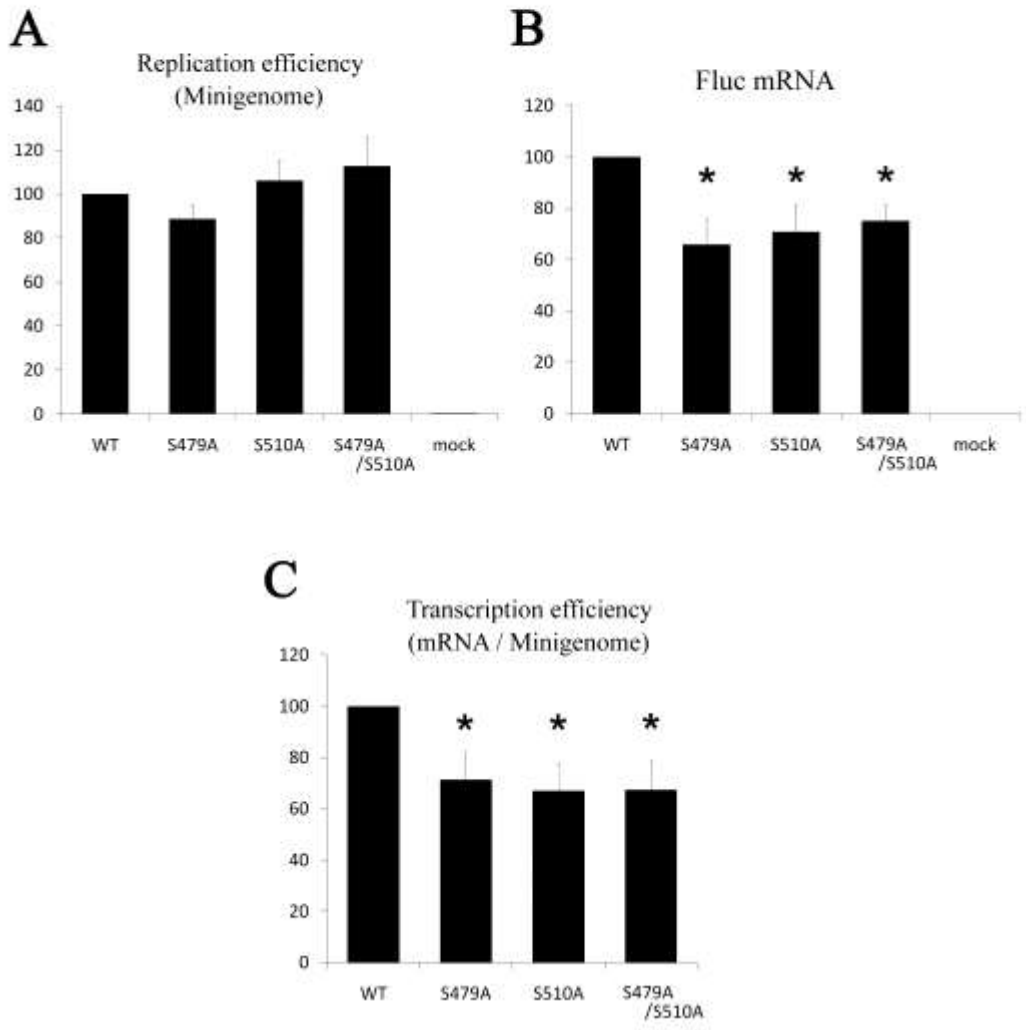

Chapter 1 - Figure 6

CHAPTER 2

Detailed Investigations for Phosphorylation Sites of Measles Virus Nucleoprotein:

Growth kinetic analysis for recombinant viruses containing mutation in the nucleoprotein phosphorylation sites

CHAPTER 2

INTRODUCTION

MV N protein associates with the viral RNA genome to form the N-RNA complex, providing a template for viral RNA synthesis. In our previous study, it has been reported that the MV N protein undergoes phosphorylation, and the major phosphorylation sites of the MV N protein are S479 and S510 (Hagiwara, *et al*., 2008). In CHAPTER 1, the author also showed that the status of the major phosphorylation sites of the N protein affected to the phosphorylation status of the P protein (Sugai, *et al*., 2012). However, the functional significance of these N-phosphorylation sites has not been clarified.

In this chapter, the author rescued recombinant MV (rMV) HL strains (Kobune, *et al*., 1996) whose phosphorylation sites in the N protein were substituted with alanine residues (rMV-S479A, rMV-S510A, and rMV-S479A/S510A) using a reverse genetics system that we had previously established (Terao-Muto, *et al*., 2008), and conducted detailed investigation for influence of their phosphorylation on virus growth.

MATERIALS AND METHODS

Cells, Viruses, Plasmids, and Antibodies

B95a cells (Epstein-Barr virus-transformed marmoset B-lymphoblastoid cells) (Kai, *et al*., 1993; Kobune, *et al*., 1996) were propagated in a RPMI-1640 medium (Sigma) supplemented with 5% fetal bovine serum (JRH Bioscience), 2 mM L-glutamine, 100 U/ml penicillin, and 0.1 mg/ml streptomycin at 37ºC/5% CO_2. HEK 293 and 293SLAM cells (HEK 293 cells stably expressing the signaling lymphocyte activation molecule [SLAM], which is a cellular receptor for MV) (Sato, *et al*., 2008; Tatsuo, *et al*., 2000) were maintained in Dulbecco's modified Eagle's medium (Sigma) with the same supplements described above. The virulent MV-HL strain (Kobune, *et al*., 1996) and its recombinant viruses were propagated and titrated in B95a cells. The generation of the pCAGGS mammalian expression vectors (Niwa, *et al*., 1991) containing wild-type N (wt-N), N mutants (S479A, S510A, S479A/S510A, and 74-77A), P, and M genes from the MV-HL strain, along with anti-N, -P, and -M polyclonal antibodies, and anti-N protein monoclonal antibody 8G were prepared as previously described (Hagiwara, *et al*., 2008; Masuda, *et al*., 2006).

Rescue of rMVs

Amplification of the MV N mutant genes (S479A, S510A, and S479A/S510A) was conducted by polymerase chain reaction (PCR) using Takara LA Taq (Takara Bio) and primers F (5′-CGG CGG CCG CTT CAC GAT GGC CAC ACT TTT GAG G-3′, *Not*I

site underlined) and R (5′-CAG GCC GGC CCT AGT CTA GAA GAT CTC T-3′, *Fse*I site underlined). The amplicons were cloned into the pCR2.1 TOPO (TOPO TA Cloning Kit, Invitrogen) vector according to the manufacturer's instructions. The resulting plasmids were transformed into *Escherichia coli* DH5α cells and grown, then digested with *Not*I and *Fse*I (Takara Bio), and fragments inserted between the *Not*I and *Fse*I sites of the MeV-HL full genomic plasmid (7+) (Terao-Muto, *et al*., 2008) to replace the wt-N gene. Rescue of the recombinant viruses was conducted as previously reported (Terao-Muto, *et al*., 2008). Briefly, vaccinia virus-infected HEK 293 cells were transfected with N, P, and L protein expression plasmids, and the MV full genome plasmid whose N protein was mutated at phosphorylation sites (pMDBI-wt, S479A, S510A, and S479A/S510A). B95a cells were added onto transfected HEK 293 cells 2 days after transfection. When an adequate cytopathic effect was observed, infected cells were subjected to three freeze-thaw cycles followed by sonication. After removal of cellular debris, recombinant viruses in the supernatant were concentrated by centrifugation (25,000 rpm, 2 h, 4ºC) in an Sw28 rotor (Beckman), and the viral pellet dissolved in an appropriate volume of phosphate-buffered saline (PBS). Viral titers were expressed as the 50% tissue culture infectious dose per milliliter ($TCID_{50}$/ml), and were measured in B95a cells. Reverse transcription (RT) and direct sequencing using viral RNA extracted from infected cells of each recombinant virus were conducted to ensure that substitutions in the phosphorylation sites were contained in the N protein gene of the recombinant viruses.

Immunoprecipitation assay

HEK 293 cells were transfected with plasmids expressing wt-N and N mutants (S479A, S510A, S479A/S510A and 74-77A), with or without the P plasmid. At 24 h post-transfection, 0.38 mCi/ml ^{32}P (Phosphorus-32 Radionuclide, PerkinElmer) or 0.06 mCi/ml ^{35}S (EasyTag Express Protein Labeling Mix, PerkinElmer) was added to the medium, and incubated at 37°C for 24 h. Cells were harvested and lysed using lysis buffer (0.5 mM EDTA, 0.5% TritonX-100 in PBS) supplemented with a Protease Inhibitor Cocktail (BD Biosciences) and a PhosSTOP Phosphatase Inhibitor Cocktail (Roche Applied Science) for 1 h at 4°C. Cell debris was removed from the lysate by centrifugation. Lysates were incubated with Protein A Sepharose CL-4B (Amersham Biosciences) and anti-N or -P polyclonal antibodies for 16 h at 4°C. Beads were washed five times with PBS, and suspended in 2× Laemmli's sodium dodecyl sulfate (SDS) sample buffer. Proteins were separated by SDS-polyacrylamide gel electrophoresis (PAGE), and radioactivity detected using an Imaging Plate and phosphorimager FLA-5100 (Fujifilm). Experiments were performed two or three times independently. The principle of the Imaging Plate method is as follows: the photostimulable phosphor on the Imaging Plate stores radiation energy by the electrical change from the ground state to the excited state. The stored excitation energy is converted to chemiluminescence by laser scanning of the phosphorimager, and the data are saved in a digital format. This detection system enables quantitative analysis of phosphorylation within a linear range.

5×10^5 293SLAM cells were infected with wild-type or rMV-HL viruses. The

author then added ^{32}P (0.38 mCi/ml) and ^{35}S (0.06 mCi/ml) to the medium just after infection, and viruses were labeled until infected cells were harvested. At each time point from 16 h post-infection (hpi) to 6 days post-infection (dpi), cells were harvested and lysed. Following immunoprecipitation, SDS-PAGE and imaging were carried out as described above.

One-step and multi-step growth kinetics

The author infected 293SLAM cells with wt or recombinant viruses at a multiplicity of infection (MOI) of 1.0 or 0.001, in duplicate. The infected cells and supernatant were harvested at 4, 8, 12, 16, 20, and 24 hpi (MOI = 1.0), or 12, 24, 48, 72, 96, 120, and 144 hpi (MOI = 0.001), respectively. After three cycles of freeze-thawing and sonication of infected cells, lysates were centrifuged to remove cellular debris, and the supernatant collected. The titer ($TCID_{50}$/ml) of each sample was measured using B95a cells.

Western blot analysis

The 293SLAM cells infected with MVs were washed in PBS and lysed in buffer (0.5 mM EDTA, 0.5% TritonX-100 in PBS) containing a Protease Inhibitor Cocktail, at 8, 16, 20, and 24 hpi (MOI = 1.0), and 2, 3, 4, 5, and 6 dpi (MOI = 0.001). The HEK 293 cells transfected with expression plasmids using the FuGENE 6 Transfection Reagent (Roche Applied Science) were lysed at 48 h post-transfection. Each lysate was separated by 8% or 10% SDS-PAGE, and transferred onto an Immobilon-P Transfer

Membrane (Millipore). Membranes were blocked with BlockACE (DS Pharma Biomedical), then incubated with a primary antibody for 1 h at 37°C. The membrane was washed five times with PBS containing 0.05% Tween-20, and incubated with a polyclonal rabbit anti-mouse IgG conjugated to horseradish peroxidase (1:2000 dilution; Dako Cytomation) for 1 h at 37°C. Immunoreactive bands were visualized using ECL western blotting detection reagents (GE Healthcare). Detection and scanning of chemiluminescence were performed with a luminescent image analyzer (LAS-1000UV mini system, Fujifilm).

Measurement of IFN-β and RANTES levels

The 293SLAM cells were infected with wt-MV or rMVs at an MOI of 1.0. Total RNA was extracted with ISOGEN (Nippon Gene) at 24 hpi, and RT was conducted with a 1:1 mixture of oligo-dT primers and random hexamers, and PrimeScript RTase (Takara) according to the manufacturer's instruction. Quantitative PCR (qPCR) assays were conducted using IFN-β-specific (5′-CAG CAG TTC CAG AAG GAG GA-3′ and 5′-AGC CAG GAG GTT CTC AAC AA-3′) and RANTES-specific (5′-TCA TCC TCA TTG CTA CTG CC-3′ and 5′-GGT GAC AAA GAC GAC TGC TG-3′) primers and SYBR Premix Ex Taq (Takara). GAPDH was used as an internal control and expression levels determined with specific primers (5′-AAC ATC ATC CCT GCC TCT ACT G-3′ and 5′-GCT TCA CCA CCT TCT TGA TGT C-3′). All qPCR assays were conducted on a Rotor-Gene Q (Qiagen).

Indirect immunofluorescence assays

The HEK 293 cells were transfected with expression vectors for wt-N, N protein mutants (S479A, S510A, S479A/S510A and 74-77A), and the P protein using the FuGENE 6 Transfection Reagent, according to the manufacturer's instructions. At 24 h post-transfection, cells were fixed with 3% paraformaldehyde in PBS, and permeabilized with 0.5% Triton X-100 in PBS. Cells were incubated with an anti-N protein polyclonal antibody, followed by incubation with AlexaFluor 488-conjugated goat anti-rabbit IgG (1:2000; Invitrogen) supplemented with Hoechst 33342 (Cambrex Bio Science). A confocal laser-scanning microscope (Fluoview FV1000-D system; Olympus) was used to visualize the fluorescence.

Complex formation assay

HEK 293 cells were transfected with plasmids expressing wt-N, N mutants, P, or M proteins. Cells were lysed at 48 h post-transfection, and the cell lysates of N, P, and M protein-transfected cells were mixed and incubated for 1 h at 4°C. N, P, and M protein complexes were immunoprecipitated with an anti-N protein monoclonal antibody 8G. Co-precipitated N, P, and M proteins were separated by SDS-PAGE and detected by immunoblotting using anti-N, -P, and -M protein polyclonal antibodies.

Pulse-chase assay

The 293SLAM cells infected with wt-MV or N protein rMVs (S479A, S510A, and S479A/S510A) at an MOI of 0.01 were labeled with [5,6-^{3}H] uridine (20 μCi/ml,

PerkinElmer) for 18 h between 6 and 24 hpi. The culture medium was replaced with medium containing excess UTP (200 nM/ml, Roche) and ribavirin (250 μM) at 1 dpi to stop the incorporation of [5,6-^{3}H] uridine. Infected cells were harvested and lysed at 0, 6, 24, and 48 h after the medium change. The released viruses were precipitated by centrifugation, and lysed with infected cells. The nucleocapsid proteins in the lysate were separated by 25–40% sucrose gradient density centrifugation at 55,000 rpm for 1 h (Sw55Ti Rotor; Beckman). A Tri-Carb 2100TR Liquid Scintillation Analyzer (PerkinElmer) was used to measure radioactivity.

RNase protection assay

The author infected 293SLAM cells with wt-MV or rMVs (S479A, S510A, and S479A/S510A) at an MOI of 0.001. Infected cells were divided into two equal portions after 5 days of incubation. One portion was lysed with micrococcal nuclease (MNase) buffer (10 mM Tris-HCL pH 7.5, 10 mM NaCl, 5 mM $MgCl_2$, 2 mM $CaCl_2$, 1% Triton X-100, 0.5% sodium DOC, BaculoGold Protease Inhibitor Cocktail [BD Biosciences], and 100 U/ml DNase) and treated with Trizol LS (Invitrogen) to extract RNA. The other portion was lysed with MNase buffer supplemented with 100 U/ml MNase for 1 h at 37°C, followed by RNA extraction with Trizol LS. From the extracted RNAs, the viral genomic RNA was quantified by RT-PCR to calculate the protection rate from MNase. The RT reaction was conducted with MV genome RT primer (5′-GGC CGT CAT GGT GGC GAA TCC TAC CTC GAC CTG TTG TTG AAT GAA GAG TTA GAA GAG TTC AC-3′) and PrimeScript RTase (Takara), according to the manufacturer's

instructions. Subsequently, qPCR assays were conducted with forward (5′-GGC CGT CAT GGT GGC GAA T-3′) and reverse (5′-TGT TCC ACG AAG ATC CT-3′) primers and SYBR Premix Ex Taq (Takara) on a Rotor-Gene Q. Genomic RNA quantities from MNase-treated and untreated samples were compared to calculate the protection rate.

RESULTS

2.1. Binding of N protein to P protein alters the phosphorylation pattern of the N protein.

In CHAPTER 1, it was suggested that the interaction between the N and P proteins affects the N protein phosphorylation status (Sugai, *et al*., 2012). The author first compared the phosphorylation status of wt-N and its phosphorylation site mutants (S479A, S510A, and S479A/S510A) in the presence or absence of the P protein (without L and minigenome RNA) in HEK293 cells. ^{32}P- or ^{35}S-labeled wt-N and N mutants with or without the P protein were immunoprecipitated with anti-N or anti-P protein antibodies, respectively. The N protein that was expressed alone showed a different phosphorylation pattern to the N protein that bound to the P protein (Fig. 1A and B), suggesting that N-P protein interaction affects the phosphorylation status of the N protein. To further evaluate these changes, the author rescued recombinant viruses whose N protein phosphorylation sites were substituted (rMV-S479A, rMV-S510A, and rMV-S479A/S510A) by reverse genetics, and investigated the phosphorylation status of the N protein in cells infected with recombinant viruses at 2 dpi. The N protein in the rMV-infected 293SLAM cells showed the same phosphorylation pattern as the N protein in co-transfected cells (Fig. 1B and C). This implies that N-phosphorylation of rMVs in the infected cells was also affected by N-P protein association.

The N protein expressed alone in cultured cells is imported into the nucleus.

However, the presence of the P protein retains the N protein in the cytoplasm (Huber, *et al*., 1991). Therefore, it is unclear whether the changes in N-phosphorylation through the N-P interaction depends upon the change in localization, or on the binding of the N and P proteins. In our previous report, a nuclear localization signal in the N protein was already identified. Thus, the author employed an N protein mutant (74-77A, referred to as mN) that localized to the cytoplasm (Sato, *et al*., 2006) to compare the phosphorylation of the wt-N and mN expressed alone or with the P protein. The phosphorylation level of the wt-N protein associated with the P protein was 37.4% of that for the free wt-N protein in HEK 293 cells (Fig. 2A). The mN protein expressed with the P protein also had a reduced phosphorylation level (35.6%) compared with the free mN protein (Fig. 2B). This indicates that the N-phosphorylation level was directly downregulated by N-P protein binding, and was not affected by the localization of the N protein.

2.2 One- and multi-step growth kinetics of rMVs.

To investigate the influence of N-phosphorylation on virus production, the author compared one- and multi-step virus growth kinetics of wt-MV and rMVs (S479A, S510A and S479A/S510A). Released and cell-associated viruses were harvested at 4–24 hpi (one-step growth) and 0.5–6 dpi (multi-step growth) and their titers determined. In the one-step analysis, rMV-S479A/S510A rapidly replicated and reached their peak titer at 20 hpi, while the wt-MV showed slower growth kinetics until 20 hpi.

The titer of wt-MV at 24 hpi was the same or slightly higher than that of rMV-S479A/S510A. In one-step growth, rMV-S479A and rMV-A510A showed moderate replication levels; however, the peak titer for rMV-S479A was the lowest. The cell-free rMVs showed similar growth kinetics to the cell-associated viruses (Fig. 3A and B). Conversely, in multi-step growth kinetics, rMV-S479A/S510A propagated most efficiently and showed higher peak titers. These titers remained high during the plateau phase of viral growth (around 3–6 dpi). The growth of rMV-S479A was lowest, while other viruses showed moderate growth levels (Fig. 3C and D). Although rMV-S479A replicated faster than wt-MV in one-step growth kinetics, it could not maintain a higher titer than the other viruses during the latter phases of multi-step growth. The different characteristics in the early and late phases of growth suggested that N-phosphorylation has multiple roles in the virus life cycle.

To investigate the influences of N-phosphorylation on viral growth, the author performed a time course analysis of N gene expression. Recombinant virus-infected 293SLAM cells were harvested at each time point, and N proteins detected by immunoblotting. Accumulation of the N protein, and growth rates were almost similar in the one-step and multi-step growth analysis (Fig. 4A and B), suggesting that the differences in growth kinetics between wt-MV and rMVs were caused by changes in viral gene expression levels. It also suggests that N-phosphorylation is involved in the regulation of viral gene expression. It has been reported that transcription of the MV N protein induces cytokine expression, such as RANTES, in a dose-dependent manner (Noe, *et al*., 1999); therefore it was also evaluated whether these changes in viral gene

expression affected induction of the host immune response. Induction of cytokines was significantly lower for wt-MV compared with rMV-S479A/S510A and rMV-S510A (Fig. 4C and D). Infection with the rMV-S479A mutant also tended to induce higher cytokine levels compared with wt-MV infections. Therefore, it can be seen that up-regulation of viral gene expression during the early phase of rMV infection was accompanied by high levels of cytokine induction.

To further evaluate the influence of N-phosphorylation on virus growth, the author investigated the relative phosphorylation levels of the N protein at each time point. From 16 hpi to 6 dpi, the relative phosphorylation level of the N protein was constant in the 293SLAM cells (Fig. 4E). During the multi-step growth analysis, viral titers at the plateau phase inversely correlated with the phosphorylation level of the N protein. Titers for the cell-free virus showed a high inverse correlation with N-phosphorylation intensity, with a coefficient of determination (R^2) of 0.82 ($P < 0.001$) at 3–6 dpi (Fig. 4F). The R^2 for the cell-associated virus was 0.69 ($P < 0.001$), and was also significantly inverse correlated (Fig. 4G). These regression curves showed exponential trend lines. The intensity of N-phosphorylation seems to have a strong influence on the plateau-phase titer during multi-step growth. Intensely phosphorylated N protein caused a reduction in viral titer during the latter phase of infection. Conversely, N-phosphorylation intensity and early-phase viral titers did not show a significant correlation, suggesting that the difference in virus growth during the early phase of infection is not caused by different phosphorylation intensities of the N-protein. Taken together, N-phosphorylation status affects virus gene expression, and

N-phosphorylation intensity affects the titers selectively during the plateau phase of multi-step growth kinetics.

2.3. Nucleocytoplasmic trafficking and N-M protein interaction are independent of N-phosphorylation.

The phosphorylation sites of the N protein are within the C-terminal tail region, and therefore the author focused on the influence of N protein C-terminal functions, such as nucleocytoplasmic transport (Sato, *et al*., 2006) and binding to the P (Bernard, *et al*., 2009) and M proteins (Iwasaki, *et al*., 2009). Our previous research identified a nuclear export signal and a nuclear localizing signal for the MV N protein. These signal sequences were prerequisites for nucleocytoplasmic transport (Sato, *et al*., 2006). The N protein is imported into the nucleus; however, its trafficking mechanism and significance have not been fully clarified. Transiently expressed wt-N, and its phosphorylation mutants in HEK 293 cells were mainly localized in nuclear foci, with no significant difference in localization observed (Fig. 5A). This suggests that nuclear trafficking of the N protein is not under the regulation of N-phosphorylation.

It is apparent that N-P protein interaction is not affected by the phosphorylation status of the N protein (Fig. 1B). The M protein also associates with the N protein tail region, and assists in virus assembly (Iwasaki, *et al*., 2009). N protein mutants and the M protein were transiently co-expressed in HEK 293 cells, and coimmunoprecipitation assay was conducted. As a result, no significant changes in N-M

association were observed among N protein mutants (Fig. 5B). Moreover, under the presence of the P protein, there was also no difference in co-immunoprecipitation of the wt-N, N mutants, P, and M proteins (Fig. 5C). To investigate the influence of other viral proteins on N, P, and M protein binding, the author conducted immunoprecipitation experiment using wt-MV- or rMV-infected cells. As with the transcription experiment, no differences were observed in N, P, and M protein interaction (data not shown). Taken together, these results indicate that nuclear trafficking of the N protein, N-P interactions, and N-M interactions are not regulated by N-phosphorylation. Alterations in growth of the rMVs were not caused by changes in these factors.

2.4. Influence of N-phosphorylation on viral RNA stability.

The viral genome tightly associates with the N protein to form the nucleocapsid and is protected from RNases and siRNAs (Bhella, *et al*., 2004; Bitko and Barik, 2001; Moyer, *et al*., 1991). The author evaluated turnover of the viral genomic and antigenomic RNAs by pulse-chase experiments to determine any differences in the encapsidation ability of the N protein. Encapsidated RNAs of rMV-S479A were rapidly degraded, while those of rMV-S479A/S510A were relatively stable compared with wt-MV or rMV-S510A (Fig. 6A). This suggested that the stability of an encapsidated RNA was affected by the phosphorylation status of the N protein. The author further analyzed the relationship between the phosphorylation of the N protein and binding to the viral genome using a nuclease protection assay. In agreement with the results of the pulse-labeling

experiments, the genomic RNA protection rate of S479A/S510A was highest, reaching 52.8%. In contrast, genomic RNAs coated with wt-N and S510A provided 30.2 and 33.4% protection, respectively. The protection rate of S479A was limited to 10.3% (Fig. 6B). The viral genome protection rate significantly correlated with viral titers during the plateau phase of multi-step growth kinetics (cell-associated virus: $R^2 = 0.66$, $P < 0.001$; cell-free virus: $R^2 = 0.91$, $P < 0.001$) (Fig. 6C). The protection rate inversely correlated with the phosphorylation level of the N protein ($R^2 = 0.96$, $P < 0.001$) (Fig. 6D). These correlations also showed an exponential relationship as in Fig. 4F and 4G, implying that the influence of N-phosphorylation on the plateau phase of multi-step growth kinetics is a result of differences in the stability of the viral genomic RNA. Collectively, the phosphorylation intensity of the N protein affects the stability of the viral genomic RNA, and the viral titer during late-phase infection strongly depends upon viral genome stability.

DISCUSSION

In CHAPTER 2, the author have demonstrated that phosphorylation of the N protein affects viral gene expression and viral genomic RNA stability. It has been reported that the P protein has two distinct binding sites for the free N protein and the N-RNA complex (Karlin, *et al*., 2003), and therefore the P protein is thought to be a carrier that binds free N proteins for delivery to the nascent replicating viral N-RNA complex for efficient encapsidation (Curran, *et al*., 1996; Leyrat, *et al*., 2011). It has also been reported that the P protein reduces non-specific binding of the N protein to cellular RNA (Curran, *et al*., 1996). Thus, the P protein seems to play important roles in supporting viral genome encapsidation; changes in the phosphorylation status of the N protein via N-P interactions may also be required for appropriate formation of the nucleocapsid. In rabies virus, it has been reported that the phosphorylation level of the N protein associated with the P protein is kept low to strengthen its affinity for viral RNA (Huber, *et al*., 1991; Wu, *et al*., 2002; Kawai, *et al*., 1999). Consistent with these findings, the author demonstrated significantly less phosphorylation of the wt-N protein associated with the P protein, compared with the highly phosphorylated wt-N protein expressed alone (Fig. 2). Hence, the P protein functions as a carrier of the N protein and seems to maintain the N protein at a lower phosphorylation state for effective encapsidation of the viral genome.

In the one-step growth experiments using rMVs, the phosphorylation of the N protein affected viral growth kinetics. The wt-MV showed delayed growth kinetics

compared with the rMVs (Fig. 3A and B). The viral titer and N protein level for the wt-MV were similarly attenuated during the early growth phase until 24 hpi (Fig. 3A, B, 4A and B). This delay in wt-MV growth can be attributed to down-regulation of viral gene expression. These results are not consistent with those that have reported in CHAPTER1. The author demonstrated that mutations of the N-phosphorylation sites (S479A, S510A, and S479A/S510A) caused down-regulation of viral transcription in a minigenome assay (Hagiwara, *et al*., 2008; Sugai, *et al*., 2012). As with these data, some past reports that investigated the function of viral protein phosphorylations have suggested these kinds of discrepancies between viral transcriptional activity and growth; mutations at constitutive phosphorylation sites of the human respiratory syncytial virus (RSV) P protein (232A/237A and 116L/117R/119L/232A/237A) did not have significant impact on viral transcription and replication in a minigenome assay, while recombinant viruses with mutated phosphorylation sites (rA2-PP2 and rA2-PP5) showed significantly reduced growth kinetics compared with wild-type virus (Lu, *et al*., 2002). High-turnover phosphorylation at S54 was not required for viral RNA synthesis and formation of N-P and P-L protein complexes in transfection experiments (Asenjo, *et al*., 2005), whereas an absence of S54 phosphorylation caused attenuation of viral titers because the S54 phosphorylation is involved in the viral uncoating step (Asenjo, *et al*., 2008). Thus, in functional analysis of viral protein phosphorylation, since it affects various steps of viral lifecycle, viral infection experiment sometimes shows different results from transfection experiment.

Past reports have demonstrated that strategic regulation of RNA synthesis is

required for effective evasion of the host defense system (Gainey, *et al*., 2008; Sun, *et al*., 2009; Fuentes, *et al*., 2010; Dillon and Parks, 2007). Likewise, the author hypothesized that wt-MV strategically down-regulated viral gene expression to evade the host defense system during the early phases of infection. It has been reported that transcription of the MV N gene causes cytokine induction in a dose- and time-dependent manner (Noe, *et al*., 1999). Additionally, inhibition of viral transcription by limited UV irradiation or ribavirin treatment reduced MV-induced cytokine expression, such as RANTES (CCL5) (Noe, *et al*., 1999; Schall, *et al*., 1988), which is thought to play an important role in response to virus infection by recruiting monocytes, macrophages, and virus-specific memory T cells (Dillon and Parks, 2007; Nakamichi, *et al*., 2005; Pazdrak, *et al*., 2002; Kujime, *et al*., 2000; Schall, *et al*., 1990). It was also reported that uncontrolled rapid viral RNA synthesis induces cell death and expression of cytokines such as interferon-β and interleukin-6 (Sun, *et al*., 2009). Thus, a negative regulatory system of viral RNA production has been reported in some viruses (Sun, *et al*., 2009; Schmid, *et al*., 2010). The author demonstrated that attenuation of wt-MV viral gene expression activity during early growth phases contributed to reduced host immune responses (Fig. 4C and D). This feature of wt-MV could be advantageous in the context of real virus infections.

On the other hand, the differences in the plateau phase of multi-step growth kinetics were inversely correlated with phosphorylation intensity of the N protein (Fig. 3C, D, and 4E). Reduction in the phosphorylation level of the N protein enhanced stability of encapsidated viral genomic RNA (Fig. 6A and B). These data indicate that

virus growth in the plateau phase is affected by stability of the encapsidated viral genomic RNA, which is in contrast to the early phases of infection. It has been previously reported that dephosphorylation of the N protein increases viral RNA encapsidation of the N protein in rabies virus (Yang, *et al*., 1999). Moreover, removal of the C-terminal tail of the N protein, which contains major phosphorylation sites, makes the nucleocapsid more rigid in MV (Schoehn, *et al*., 2004). These data suggest that the negatively charged N protein and the viral genomic RNA repel each other and that this electrostatic repulsion weakens encapsidation of the viral genome. Therefore, excessive phosphorylation of the N protein interferes with the rapid assembly and/or strong association of the N-RNA complex. During one-step growth kinetics, total phosphorylation intensity of the N protein and viral genome stability do not have a strong impact on virus production (Fig. 3A and B). During an MV infection, the genomic RNA mainly replicates at around 12–24 hpi, and accumulates exponentially during this phase (Plumet, *et al*., 2005). Because an adequate amount of genomic RNA was supplied during this phase, viral RNA stability does not have a strong influence during the early phases of infection. In contrast, viral genome replication is restricted to the latter phases of infection. Hence, viral genome stability has a strong selective effect on the late phase of multi-step growth kinetics.

In the present study, the author demonstrated that N-phosphorylation affected viral growth by altering viral gene expression and genomic RNA stability, whereas nucleocytoplasmic transport of the N protein (Fig. 5A), N-P interactions (Figs. 1B and 5C), and N-M interactions (Fig. 5B and C) remained unaltered. During the early phases

of infection, proper phosphorylation of the N protein controls viral gene expression, and this regulation was required for efficient evasion of the host immune response. Phosphorylation intensity of the N protein at plateau growth phases regulates viral genome stability, and these data provide new insights into the machinery regulating post-replication viral RNAs. The N protein may regulate its own phosphorylation (S479 and S510), thereby optimizing its function at each step of the viral life cycle for efficient viral propagation. Further analysis of the phosphorylation and dephosphorylation mechanisms of the N protein would help our understanding of the biological significance of N protein phosphorylation regulation.

FIGURE LEGENDS

Fig. 1

Phosphorylation status of wt-N protein and phosphorylation mutants (S479A, S510A, and S479A/S510A) under various conditions. (A) HEK 293 cells were transfected with pCAGGS expression vectors encoding wt or mutant N proteins. N proteins expressed alone in HEK 293 cells were labeled with ^{32}P or ^{35}S and precipitated with an anti-N polyclonal antibody. (B) N proteins were transiently expressed with the P protein in HEK 293 cells, labeled with ^{32}P or ^{35}S, and co-immunoprecipitated with the P protein using an anti-P polyclonal antibody and quantified. (C) 293SLAM cells were infected with wt or rMVs (rMV-S479A, rMV-S510A, and rMV-S479A/S510A) at an MOI of 0.001, and labeled with ^{32}P or ^{35}S. The bar graphs below each image represent relative phosphorylation levels (^{32}P-N/^{35}S-N) for each N protein.

Fig. 2

Phosphorylation of free N protein (N^0) and P-associated N protein. (A) HEK 293 cells transiently expressing wt-N protein, with or without the P protein, were labeled with ^{32}P or ^{35}S, and immunoprecipitated with anti-N or anti-P antibodies as appropriate. The bar graph shows the relative phosphorylation levels (^{32}P-N/^{35}S-N) of the N protein. Error bars indicate standard deviations. $^{**}P < 0.01$. Location of the wt-N protein was shown by immunofluorescence using the anti-N monoclonal antibody 8G (Masuda, *et al.*, 2006), with nuclei stained with Hoechst 33342. (B) The same experiment was

conducted using an N protein mutant (mN, 74-77A).

Fig. 3

One- and multi-step growth kinetics of rMVs. 293SLAM cells were infected with wt-MV or rMVs (rMV-S479A, rMV-S510A, and rMV-S479A/S510A) at an MOI of 1.0. Cells were harvested at 8, 12, 16, 20, and 24 hpi, and titrations ($TCID_{50}$/ml) of the cell-free virus (A) and cell-associated virus (B) conducted. 293SLAM cells infected with the rMVs at an MOI of 0.001 were harvested at 12, 24, 48, 72, 96, 120, and 144 hpi, and the titers of cell-free virus (C) and cell-associated virus (D) measured.

Fig. 4

Viral N protein accumulation of wt-MV and rMVs, and their phosphorylation status. (A) 293SLAM cells were infected with wt-MV and rMVs (rMV-S479A, rMV-S510A, and rMV-S479A/S510A) and lysed at 8, 16, 20, and 24 hpi (MOI = 1.0), or at 2, 3, 4, 5, and 6 dpi (MOI = 0.001). Lysates were subjected to 10% SDS-PAGE and immunoblotting with an anti-N polyclonal antibody. (B) Relative expression levels (nucleoprotein/GAPDH) of wt-N and phosphorylation mutants of the N protein. (C) IFN-β induction and (D) RANTES induction by wt-MV and rMVs. $^{*}P < 0.05$, $^{**}P < 0.01$. (E) Relative phosphorylation levels of wt-N and N mutants in 293SLAM cells at each time point. (F and G) Correlation between phosphorylation level of the N protein and plateau-phase viral titers (3–6 dpi) during multi-step growth kinetics (cell-free and cell-associated virus). R^2, coefficient of determination; *P*, *P*-value.

Fig. 5

Nucleocytoplasmic trafficking and N-M protein interaction are not regulated by N-phosphorylation. (A) HEK 293 cells were transfected with vectors encoding wt or N protein mutants. Locations of N proteins were visualized using an anti-N antibody. Nuclei were stained with Hoechst 33342. (B) Transiently expressed N protein and its phosphorylation mutants (S479A, S510A, and S479A/S510A) complexed with the M protein in HEK 293 cells were co-immunoprecipitated with an anti-M polyclonal antibody. Precipitated N and M proteins were detected with anti-N and anti-M polyclonal antibodies, respectively. (C) HEK 293 cells were transfected with plasmids encoding the N, P, and M proteins. Expressed proteins were precipitated with anti-N monoclonal antibody and detected by immunoblotting using anti-N, -P, and -M polyclonal antibodies.

Fig. 6

Phosphorylation intensity of the N protein inversely correlated with viral genome stability. (A) 293SLAM cells were infected with wt-MV or rMVs (S479A, S510A, and S479A/S510A) at an MOI of 0.01. Infected cells were pulse chased with tritium. Cells and supernatants were collected at 0, 6, 24, and 48 h after labeling, and radioactivity measured. (B) 293SLAM cells were infected with wt-MV or rMVs, and each N-RNA complex in the cell lysate was treated with MNase. Viral genomic RNA of MNase treated, or untreated samples were quantified by RT-PCR. Error bars indicate standard

deviations. $^{**}P < 0.01$; n.s., not significant. (C) Correlation between viral genome protection rate and viral growth of wt or mutant MVs. (D) Viral genome protection rate and the phosphorylation level of N proteins.

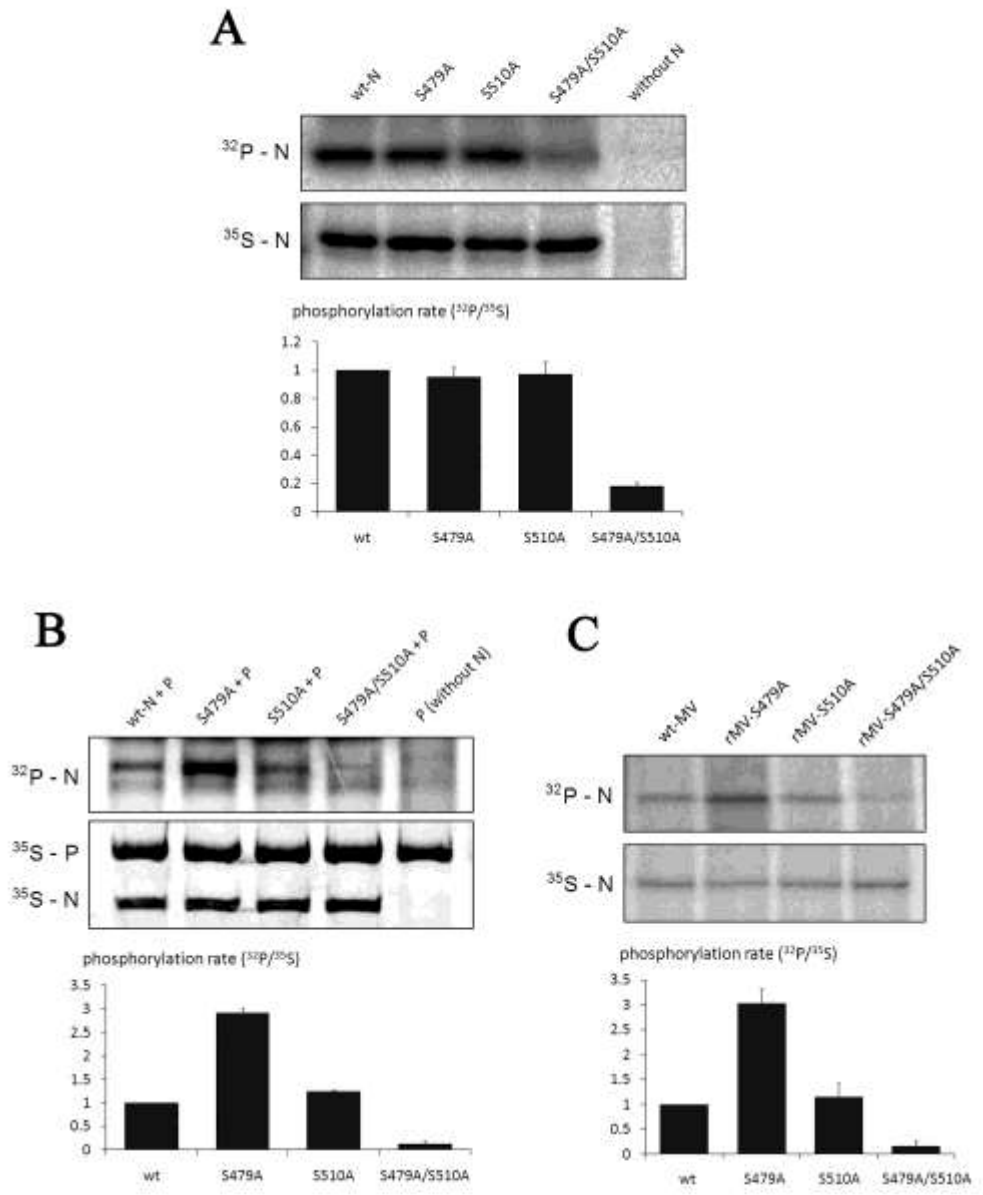

Chapter 2 - Figure 1

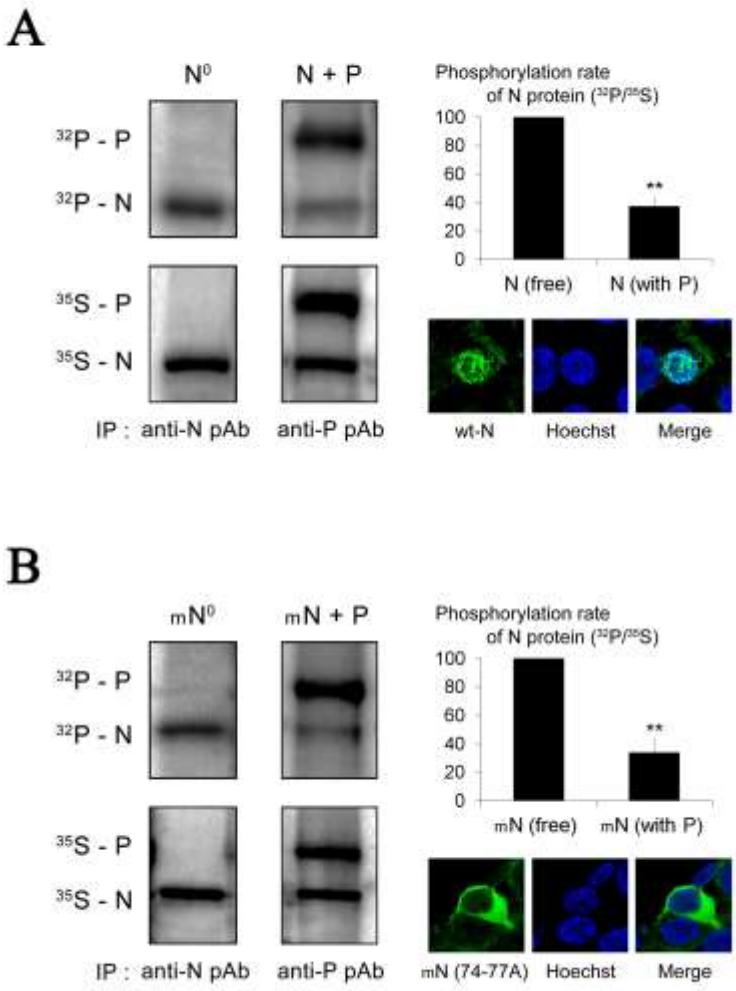

Chapter 2 - Figure 2

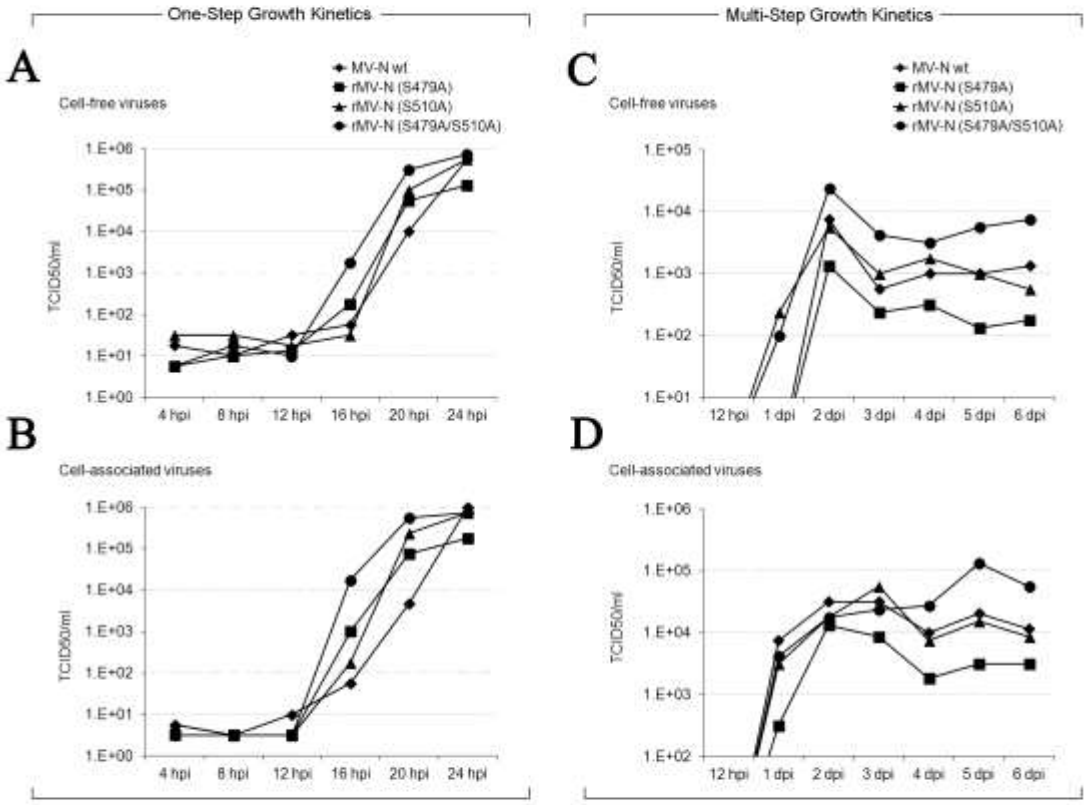

Chapter 2 - Figure 3

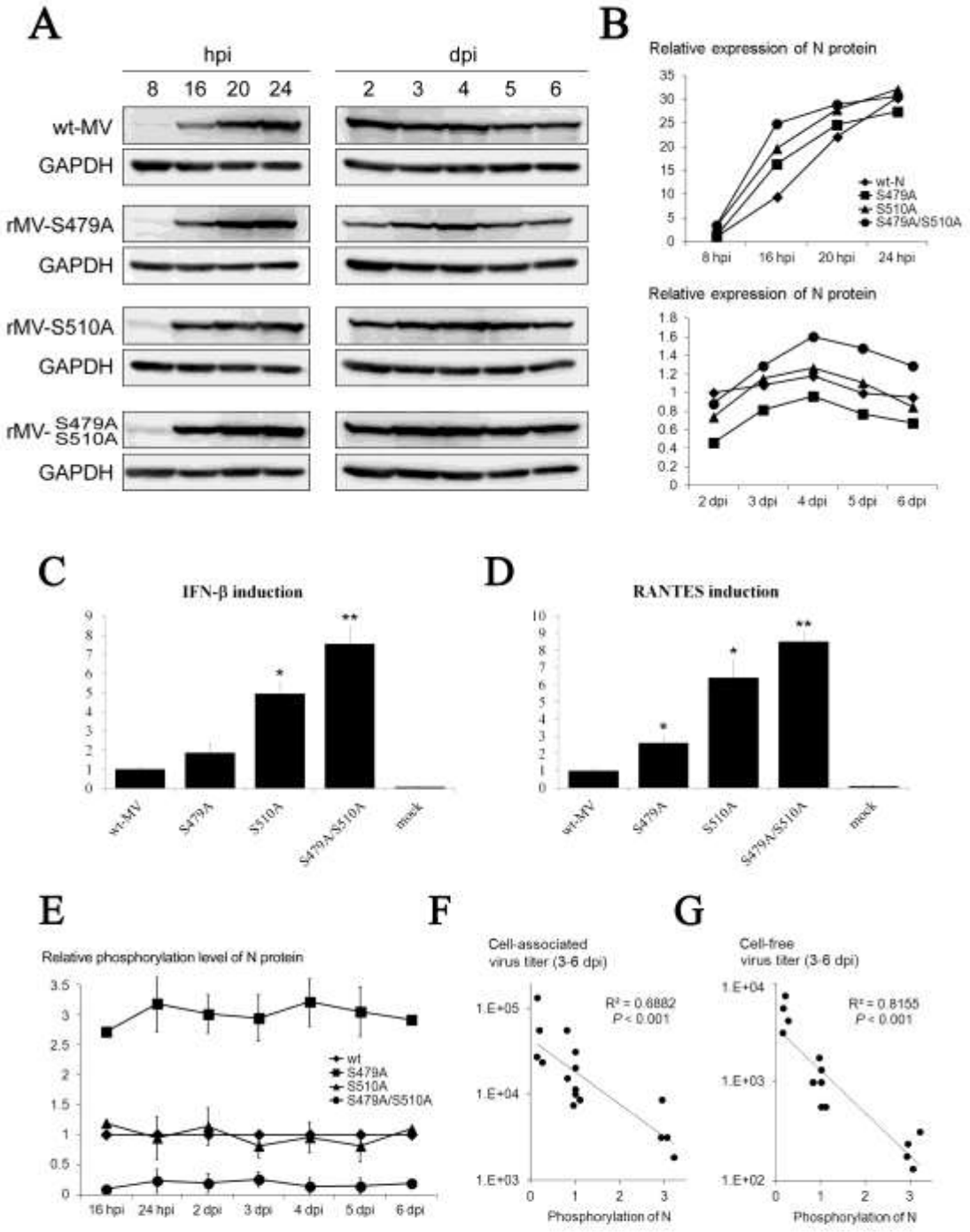

Chapter 2 - Figure 4

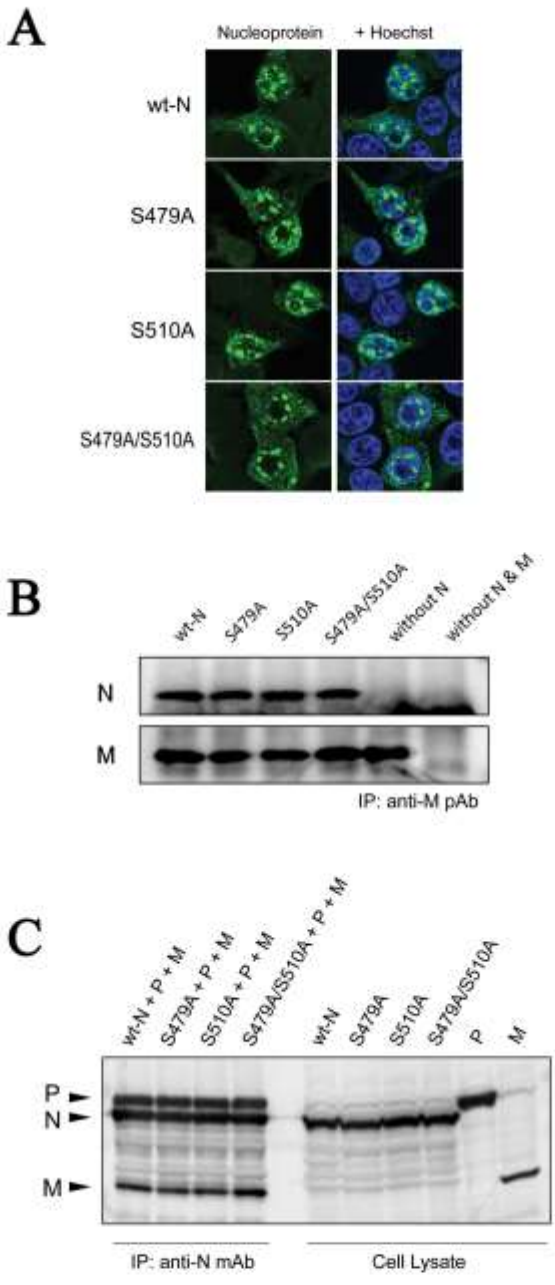

Chapter 2 - Figure 5

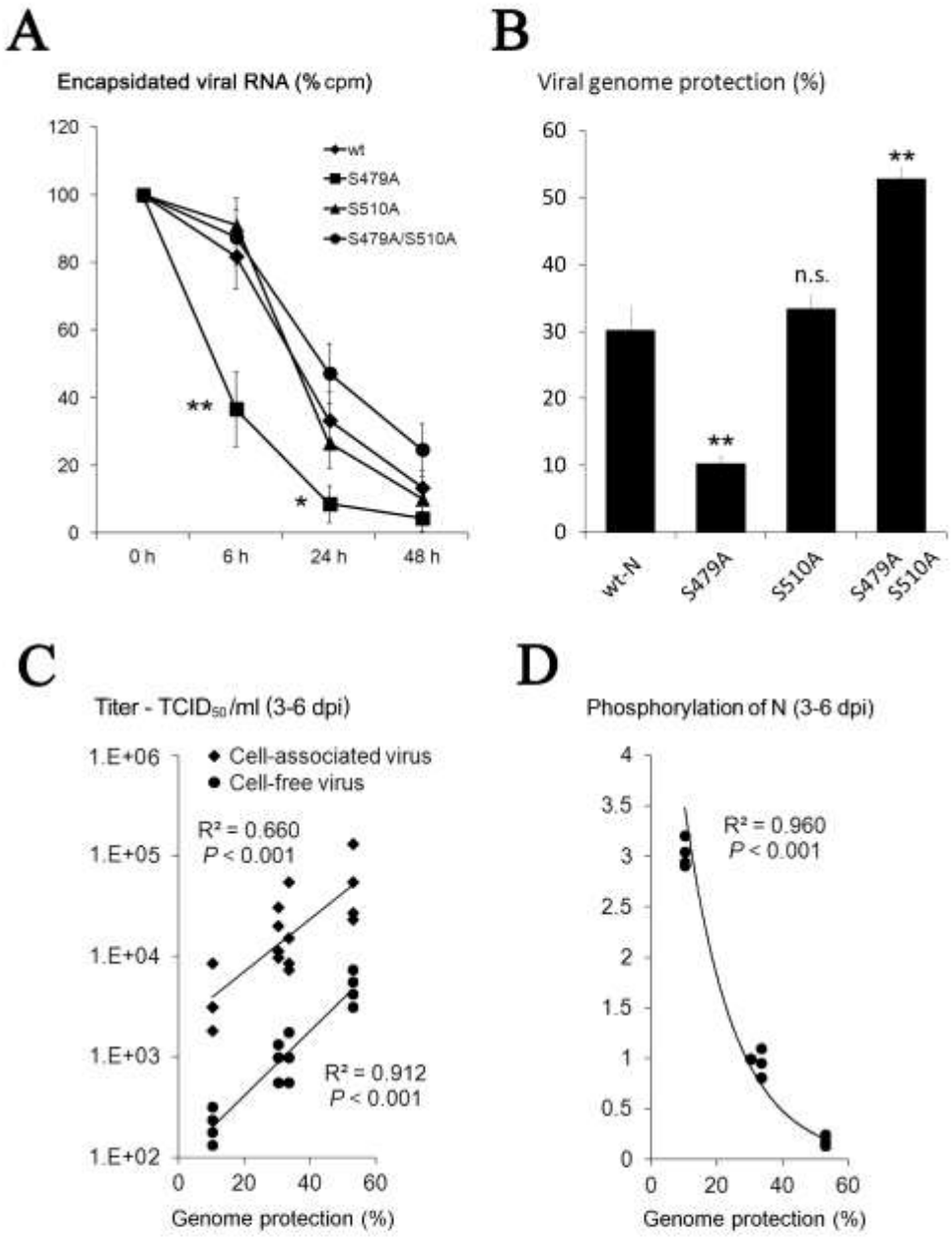

Chapter 2 - Figure 6

CHAPTER 3

Novelly Identified Phosphorylation Site of Nucleoprotein:

Nucleocapsid assembly of measles virus requires a phosphorylation modification on the core domain of nucleoprotein

CHAPTER 3

INTRODUCTION

The most defined role of MV N protein is encapsidation of viral genomic and antigenomic RNA (Bitko and Barik, 2001; Moyer, *et al*., 1990), where N proteins tightly associate with the viral genome to form an N-RNA complex that is template for viral transcription and replication (Rima and Duprex, 2009). In the CHAPTER 1 and 2, the author have demonstrated that the major phosphorylation sites of N protein (S479 and S510) are involved in various stages of the viral life cycle such as viral gene expression, virus growth rate, and viral genome RNA stability (Sugai, *et al*., 2013; Sugai, *et al*., 2012; Hagiwara, *et al*., 2008). However, despite double mutation of the major phosphorylation sites of MV N protein, it was still phosphorylated, albeit to a lesser extent (Sugai, *et al*., 2012). This suggested that the N protein had unidentified phosphorylation site. Moreover, it has been reported that N protein undergoes phosphorylation at both serine and threonine residues, and the phosphorylation intensity of the phosphothreonine was weaker than for the phosphoserine (Gombert, *et al*., 1995; Robbins, *et al*., 1980; Robbins and Bussell, 1979); this also indicated that there was unidentified novel phosphothreonine residue within the N protein. This minor phosphorylation residue has yet to be identified, and their functions are poorly understood.

In this chapter, the author predicted nine putative phosphorylation sites within the N protein by mass spectrometry (MS) analyses, and identified new phosphorylation site of N protein using alanine substitution mutants for each putative phosphorylation

site. Furthermore, the role of the new phosphorylation site in viral reproduction was examined. Here, the author demonstrated that phosphorylation at T279 is functionally indispensable for nucleocapsid formation.

CHAPTER 3

MATERIALS AND METHODS

Cells, plasmids and antibodies

Cos7, 293, 293T, and Vero cells were propagated in Dulbecco's modified Eagle's medium (DMEM) (Sigma) supplemented with 5% fetal bovine serum (JRH Bioscience), 2 mM L-glutamine, 100 U/ml penicillin, and 0.1 mg/ml streptomycin at 37°C in 5% CO_2. COBL cells were maintained in a RPMI-1640 medium (Sigma) with the same supplements as described above. pCAGGS mammalian expression vectors (Niwa, *et al*., 1991) encoding wild-type N (wt-N), N mutants, and P genes from the HL strain of MV (Kobune, *et al*., 1996) were prepared as described previously (Sugai, *et al*., 2012). Generation of a polyclonal anti-MV N antibody has also been described previously (Hagiwara, *et al*., 2008).

Matrix-assisted laser desorption/ionization/time-of-flight (MALDI-TOF/ TOF) MS analysis

MV-infected COBL cells were lysed, and NC-associated N proteins were purified by cesium chloride (CsCl) gradient centrifugation as described below. The N protein was separated by SDS-PAGE and stained with Coomassie brilliant blue. The band corresponding to the N protein was excised from the gel and destained five-times with 50 mM NH_4HCO_3 in 50% methanol. The N protein was then subjected to in-gel digestion with trypsin or V8 protease at 37°C for 16 h as previously described (Hagiwara, *et al*., 2008; Huang, *et al*., 2011). The digested peptides of N protein were

separated by nanoflow liquid chromatography (LC) (KYA Technologies Corporation) and analyzed by MALDI-TOF/TOF MS (4700 proteomics analyzer) as described previously (Hagiwara, *et al*., 2008). Detected peptides were identified by a database search using MASCOT ver. 2.0 (Matrix Science).

Immunoprecipitation Assay

Cos7, 293T, and Vero cells were transfected with plasmids containing wt-N and N mutants. At 24 h post-transfection, 0.38 mCi/ml of ^{32}P (phosphorus-32 radionuclide, PerkinElmer) or 0.06 mCi/ml of ^{35}S (EasyTag Express Protein Labeling Mix, PerkinElmer) was added to the media, and incubated at 37°C for 24 h. Cells were harvested and lysed in lysis buffer, 0.5 mM EDTA and 0.5% Triton X-100 in phosphate buffered saline (PBS) supplemented with Protease Inhibitor Cocktail (BD Biosciences) and PhosSTOP Phosphatase Inhibitor Cocktail (Roche) for 1 h at 4°C, and cell debris was removed from the lysate by centrifugation. The lysate was incubated with protein A sepharose CL-4B beads (Amersham Biosciences) and anti-MV N polyclonal antibody for 16 h at 4°C. The beads were collected, washed 5 times with PBS and suspended in 2× Laemmli's sample buffer. Component proteins were separated by SDS-PAGE, and detected by radioactivity using an Imaging Plate and phosphorimager FLA-5100 (Fujifilm).

Minigenome expression assay

Precise methods for the minigenome experiment were described previously (Sugai, *et*

al., 2012). Briefly, 293 cells in 24-well plates were transfected with N, P, and L protein expression plasmids using Lipofectamine LTX Reagent (Invitrogen) and Plus Reagent (Invitrogen). After 24 h, viral minigenomic RNA encoding the firefly luciferase gene were transfected with Lipofectamine 2000 Reagent (Invitrogen). The following day, cells were lysed in Passive Lysis Buffer (Promega), and luciferase activity was measured using a PicaGene Luminescent Kit (Tokyo Ink Manufacturing) according to the manufacturer's instructions. Fluorescence intensity was detected by Mini Lumat LB 9506 (Berthold).

N-P protein binding assay

Cos7 cells were transfected with either wt-N or mutant N protein (T279A) expression plasmids, and a P protein expression plasmid using Lipofectamine LTX Reagent and Plus Reagent. The following day, cells were labeled with ^{35}S (0.06 mCi/ml) at 37°C for 24 h. The cells were lysed, and the lysate was incubated with Protein-A Sepharose CL-4B and anti-N protein antibody. The precipitated proteins were separated by SDS-PAGE and detected with phosphorimager FLA5100.

Indirect immunofluorescence assay

Cos7 cells were transfected with expression vectors for wt-N, N protein mutants (T279A, T279D, T279E, S479A/S510A, ST8A, and ST11A), and P protein using FuGENE 6 Transfection Reagent according to the manufacturer's instructions. At 24 h post-transfection, cells were fixed and permeabilized with 3% paraformaldehyde/PBS

and 0.5% Triton X-100/PBS, respectively. The cells were incubated with polyclonal anti-N protein antibody and monoclonal anti-P protein antibody followed by incubation with 1:2000 dilution of Alexa Fluor 488 F(ab')2 fragment of goat anti-rabbit IgG (H+L) (Invitrogen) and Alexa Fluor 568 F(ab')2 fragment of goat anti-mouse IgG (H+L) (Invitrogen) supplemented with Hoechst 33342 (Cambrex Bio Science). Fluorescence was visualized by confocal laser scanning microscope Fluoview FV1000-D system (Olympus).

Nucleocapsid purification

Cos7 cells were transfected with the expression plasmid for N protein or its mutants using FuGENE 6 Transfection Reagent (Roche Applied Science) according to the manufacturer's instructions. At 48 h post transfection, cells were lysed in TNE buffer (10 mM Tris (pH 7.8), 150 mM NaCl, and 1 mM EDTA) supplemented with 1% NP40 and Protease Inhibitor Cocktail at 4°C for 30 min. The lysate was layered onto 1.5 ml each of 25%, 30%, and 40% CsCl (w/v) gradients in TNE buffer and centrifuged in a Beckman Sw55Ti rotor for 2 h at 55,000 rpm. The fraction containing the nucleocapsid was diluted with TNE and centrifuged at 55,000 rpm to precipitate the nucleocapsid, which was resolved in an appropriate volume of PBS.

Western blot analysis

Expression plasmids for wt-N and T279A were transfected in Cos7 cells, and each cell lysate was subjected to western blot analysis to detect expression levels of the N protein

relative to an internal control, GAPDH. The cell lysates were then separated by CsCl gradient centrifugation. The NC fraction was collected and further centrifuged to precipitate the NC-like particles. The yields of the NC-like particles were also visualized and quantified by western blotting. Briefly, the lysate of N protein transfected cells and purified nucleocapsids were subjected to 10% SDS-PAGE, and the separated proteins were transferred onto Immobilon-P Transfer Membrane (Millipore). The membrane was blocked with BlockACE (DS Pharma Biomedical), and then incubated with anti-N polyclonal antibody for 1 h at 37°C. The membrane was washed five times with 0.05% Tween/PBS and incubated with 1:2000 dilution of polyclonal goat anti-rabbit horseradish peroxidase-conjugated immunoglobulins (Dako Cytomation) for 1 h at 37°C. Immunoreactive bands were detected using ECL Western blotting detection reagents (GE Healthcare). Scanning of chemiluminescence was performed with a luminescent image analyzer LAS-1000UV mini system (Fujifilm).

Electron microscopy

Cos7 cells were transfected with wt-N or N-T279A expression plasmids using Plus Reagent and Lipofectamine LTX Reagent, and self-assembled NC-like particles were purified 2 days post-transfection. Sample preparation for the electron microscopy was performed as previously described (Hagiwara, *et al.*, 2008). Briefly, purified NC-like particles were spotted on a copper grid coated with collodion, and incubated for 5 min at room temperature. The samples were then negative-stained with 2% uranyl acetate, and observed under an electron microscope H7000 (Hitachi).

Limited Proteolysis

Purified NC fraction of wt-N, N-T279A, and heat-denatured wt-N (for 10 min at 95°C) were equally divided into eight tubes, and each aliquot was subjected to 0, 0.1, 0.25, 0.5, 1.0, 2.5, 5.0, or 10.0 μg/ml of trypsin treatment for 1 h at 37°C. The reactions were stopped by adding SDS sample buffer and heating for 5 min at 95°C, and then subjected to SDS-PAGE. The proteolytic bands were detected by immunoblot using anti-N polyclonal antibodies.

Bacterial alkaline phosphatase (BAP) treatment and NC fractionation

Cos7 cells in 6-cm dishes were transfected with expression plasmids for wt-N, N-T279A, and ST10A using FuGENE 6 Transfection Reagent. At 24 h post-transfection, the nucleocapsids were purified by CsCl gradient centrifugation and dissolved in 200 mM Tris-HCL buffer (pH 8.0) supplemented with Protease Inhibitor Complete EDTA-free (Roche Diagnostics). Each sample was incubated with or without 1.5 units of BAP and PhosSTOP Phosphatase Inhibitor Cocktail for 2 h at 65°C, and then 500 mM NaCl was added and incubated for 1 h at 37°C. NC-like particles were separated by CsCl gradient centrifugation (0.6 ml of 30% glycerol (v/v), 1.2 ml of 20%, 1.4 ml of 30%, and 1.4 ml of 40% CsCl (w/v) in TNE buffer) in a Beckman Sw55Ti rotor for 16 h at 36,000 rpm, and the gradients were divided into seven fractions. N proteins contained in each fraction were immunoprecipitated with Protein A Sepharose CL-4B and anti-N polyclonal antibodies, and were subjected to SDS-PAGE and western

blot analysis to quantify N protein levels.

RESULTS

3.1. Identification of a novel phosphorylation site within MV-N protein.

In our previous paper, MALDI-TOF/TOF MS and ESI-Q-TOF MS analysis of MV-N protein was conducted, and two major phosphorylation sites were identified from the tryptic peptides of N protein purified from N-plasmid transfected cells (Hagiwara, *et al*., 2008). However, minor phosphorylation sites of N protein were not identified from these tryptic peptides. Therefore, in this study, the author re-examined minor phosphorylation of the N protein by MALDI-TOF/TOF MS analysis using trypsin digested N protein derived from MV-infected cells. Additionally, investigation of the minor phosphorylation was performed using V8 protease-digested N protein. In the latter case, phosphorylated peptides were selectively detected and analyzed by MALDI-TOF/TOF MS. As a result, the peptides digested with trypsin or V8 protease covered 70.5% of the N protein sequence (Fig. 1A and 1B), and nine putative phosphorylation sites were predicted: T279, S294, S295, S407, S418, T454, S456, S457, and S460. The author further investigated these putative phosphorylation sites to identify responsible sites for the minor phosphorylation of N protein. The author prepared alanine substitution mutants for each putative phosphorylation site of N protein, and examined phosphorylation levels of each putative phosphorylation site by ^{32}P labeling and immunoprecipitation. Mutants used in this study are shown in Fig. 2A. As a result, the T279 site was remarkably phosphorylated among these nine putative

phosphorylation sites, with a phosphorylation rate of 14.3% for wt-N protein in Cos7 cells (Fig. 2B). The phosphorylation rate of T279 in Vero and 293T cells was also investigated, but did not observe a significant change in these cells compared with Cos7 cells (Fig. 2C). This indicated that the minor phosphorylation at T279 was not cell-type specific phenomenon. Phosphorylation at the eight remaining putative phosphorylation sites occurred at trace level, and therefore these sites may not be phosphate group acceptors. Additionally, phosphorylation signals were barely detected in ST11A, where two major and nine minor putative phosphorylation sites were alanine-substituted.

The *Paramyxovirus* N protein possesses a highly conserved domain at amino acids (aa) 258-357 which is referred to as the central conserved region (CCR) (Fig. 3A), and is known to be important for N protein function (Liston, *et al*., 1997; Karlin, *et al*., 2002). In previous (Hagiwara, *et al*., 2008) and present MS analysis (Fig. 1), aa 250-278 and 298-324 were not covered within the N protein CCR. This region includes six serine and threonine residues: T259, S268, T272, S298, T309, and S319. The author generated additional alanine mutants, named ST14A and ST17A (Fig. 3B), and examined whether the slight phosphorylation levels in ST11A were responsible for these sites. Phosphorylation of ST14A and ST17A was similar to that for ST11A (Fig. 3C), suggesting that these six sites within CCR were not phosphate group acceptors. Trace level phosphorylation which was detected in ST11A, ST14A, and ST17A appeared to be non-specific phosphorylation that occurs at very low rates.

3.2. T279 is an essential phosphorylation site for N protein function.

To identify the phosphorylation sites required for N protein function from the nine putative sites, the author prepared alanine-substituted mutants of N protein and measured each N protein activity by minigenome reporter assay. In agreement with the previous data, a double mutant of the major phosphorylation sites S479A/S510A showed 46.3% activity compared with that for the wt-N protein (Fig. 4A), whereas an alanine substitution mutant of the T279 site showed a complete loss of activity and did not aid transcription and replication, indicating the T279 site is functionally important. Alanine substitution mutant at the eight putative phosphorylation sites other than T279 (ST8A) showed no reduction in activity compared with wt-N protein. Additionally, the activity of an ST10A mutant (where two major phosphorylation sites and eight putative phosphorylation sites other than T279 were substituted with alanine) reduced activity to 36.6%. There was no statistically significant difference between S479A/S510A and ST10A activity. Thus, the eight putative phosphorylation sites other than T279 were not required for N protein function, but the T279A mutant was functionally indispensable. Therefore, the author investigated the T279 site further using N protein mutants whose T279 sites were substituted with aspartic acid (D) and glutamic acid (E). The T279D and T279E mutants showed no activity similar to the T279A mutant in the minigenome assay (Fig. 4B). Since substitutions of T279 to acidic residues did not mimic the phosphorylation of T279, constitutively charged T279 may be undesirable for N protein function.

The N protein possesses a nuclear localization signal and nuclear export

signal for nucleocytoplasmic transport, and the N protein expressed alone in cultured cells localizes to the nucleus (Sato, *et al*., 2006; Huber, *et al*., 1991). To investigate the significance of the T279 site, the localization of the putative phosphorylation site mutants including a series of T279 mutants were examined by indirect fluorescent antibody (IFA) assay. The N protein mutants S479A/S510A, ST8A, and ST10A showed nuclear localization identical to wt-N protein, while T279 mutants showed diffuse cytoplasmic distribution (Fig. 5A and B). Thus, T279 mutants showed abnormal properties by IFA assay. The P protein has been known to retain N protein in the cytoplasm and co-localizes with the N protein (Huber, *et al*., 1991). Under the presence of the P protein, the T279A mutant exhibited a dotted co-localization pattern with the P protein in the cytoplasm, similar to that seen for the wt-N protein (Fig. 5C).

P protein is a major binding protein of the N protein and is required for viral transcription and replication (Bernard, *et al*., 2009; Bourhis, *et al*., 2005). The P protein functions as a carrier of the N protein to nascent replicating viral N-RNA complexes for efficient encapsidation (Curran, 1996), stabilizes NC by regulating the phosphorylation status of N protein (Sugai, *et al*., 2013), and prevents nonspecific binding of the N protein to host cellular RNA (Curran, 1996). To probe the mechanism of deactivation for the T279A mutant in a minigenome assay, the binding abilities of wt-N and T279A to P protein were investigated by co-immunoprecipitation assay. Transiently expressed wt-N or T279A with P protein were labeled with ^{35}S, and immunoprecipitated using anti-N polyclonal antibodies. There were no differences in co-precipitation of the P protein (Fig. 5D); this finding and dotted co-localization with P protein (Fig. 5C)

suggests that T279A mutant possesses normal binding ability with P protein, and therefore loss of activity of the T279A mutant in the minigenome assay was independent of N-P interactions.

3.3. T279 phosphorylation site of N protein is a prerequisite for NC formation.

The region around T279 of MV-N protein is called CCR and has been reported to function as an N-N and N-RNA interaction domain to form NCs (Karlin, *et al*., 2002; Myers, *et al*., 1999; Terao-Muto, *et al*., 2008). Multiple sequence alignment of CCR among *Paramyxoviridae* revealed that T279 is highly conserved (Fig. 3A). Therefore, the author examined whether the T279 phosphorylation site was required for NC formation. NC formation ability was tested by measuring and comparing the amount of NC-like particles in N plasmid transfected cells between the wt-N and T279A mutant. The expression of wt-N protein and T279A in Cos7 cells were similar, while purified NC-like particles from T279A transfected cell lysates were significantly reduced compared with wt-N protein (Fig. 6A). Thus, alanine substitution at T279 caused a remarkable impairment of NC formation, and the T279 mutants showed a loss of activity in the minigenome assay.

Of note, the T279A mutants were detected in the NC fraction in CsCl gradient centrifugation experiment (Fig. 6A), although the T279A mutant lost activity in the minigenome assay (Fig. 4A). To clarify that the N proteins acquired from the NC fraction formed correct NC structures, the author subjected them to electron microscopy.

The wt-N protein showed a typical herringbone structure, while the T279A mutant from the NC fraction did not form a correct NC structure, and various sized aggregates were detected (Fig. 6B), suggesting that the T279A mutant did not retain the ability of self-assembly and/or RNA encapsidation.

Furthermore, the author generated a full-genomic plasmid containing the T279A mutation in the N protein and attempted to rescue the T279A recombinant virus using a reverse genetics system that we had previously established (Sugai, *et al*., 2013; Terao-Muto, *et al*., 2008; Myers, *et al*., 1997). However, we were unable to rescue the T279A mutant virus. This seems to be attributed to a loss of N protein functions; the T279A mutant nucleoprotein could not correctly encapsidate the RNA (Fig. 6B) and did not support viral transcription and replication (Fig. 4A and B).

3.4. Phosphorylation modification at T279 is required for NC formation.

N protein consists of a highly structured N-core domain (aa 1-400) and an intrinsically disordered N-tail domain (aa 401-525) (Sato, *et al*., 2006; Bourhis, *et al*., 2005). A correctly folded N-core domain is resistant to proteases including trypsin (Myers, *et al*., 1997; Heggeness, *et al*., 1981). The tertiary structure of the T279A mutant was evaluated by limited proteolysis to determine whether the loss of self-assembly was due to the decay of N-core conformation or absence of phosphorylation. Plasmids for wt-N and T279A were transfected into Cos7 cells, and each N protein was purified from the NC fraction of CsCl gradient centrifugation. The purified N proteins were subjected to

limited proteolysis with various concentrations of trypsin. Indeed, the 43.5 kDa core domain of the wt-N protein was resistant to trypsin hydrolysis (Fig. 7A). Heat-denatured wt-N protein showed a different degradation pattern, and various proteolytic products less than 43.5 kDa were detected (Fig. 7B). The T279A mutant showed trypsin resistance, and its degradation pattern was identical to that of wt-N protein (Fig. 7C). These results imply that the tertiary structure of the core domain of the T279A mutant retained structural integrity. Thus, alanine substitution of T279 did not cause denaturation of the tertiary structure of N-core domain, but absence of the T279 phosphorylation seemed to be critical for NC formation.

To investigate the significance of T279 phosphorylation on NC formation, the author conducted dephosphorylation of T279 with BAP and examined whether this caused abnormalities in NC formation. Previous reports demonstrated that deficient NC-like particles could be discriminated by CsCl centrifugation in Sendai virus (Myers, *et al*., 1999; Myers, *et al*., 1997; Buchholz, *et al*., 1993). Using the same conditions, the author examined whether this method was applicable to MV-N protein. The wt-N and T279A transfected cell lysates were subjected to CsCl gradient centrifugation to discriminate between normal and deficient NC-like particles. The gradients were divided into seven fractions, and N protein in each fraction was detected by western blot. The NC-like particles of wt-N were mainly detected in fraction 6 to 7 (Fig. 8A), while aggregates of the T279A mutant were broadly detected from fraction 1 to 7 (Fig. 8B) indicating the deficient NC-like particles formed various size aggregates. Thus, normal NC-like particles could be discriminated from deficient aggregates. To demonstrate that

T279 phosphorylation is important in NC formation, the author then evaluated the influence of dephosphorylation of the ST10A mutant by examining whether the ST10A mutant could form normal NC-like particles in the presence or absence of BAP. All phosphorylation sites other than T279 are substituted with alanine residues in the ST10A mutant (Fig. 2A). Since there are no significant phosphorylation sites other than the 11 sites (Fig. 2B, 3B, and 3C), the influence of the BAP treatment on ST10A is equivalent to T279 dephosphorylation. NC-like particles from ST10A were mainly detected in NC fractions 6 to 7, similar to the intact NC-like particles, suggesting ST10A formed normal NC-like particles (Fig. 8C). ST10A with BAP treatment showed a wide distribution from fractions 2 to 7 (Fig. 8D), indicating that dephosphorylation of T279 caused a deficiency in NC formation. Furthermore, addition of a phosphatase inhibitor abrogated the NC deficiency caused by BAP treatment (Fig. 8E) indicating it was not caused by binding of BAP to N protein but by dephosphorylation at T279. Taken together, these results suggest that phosphorylation at T279 is a prerequisite for NC formation.

DISCUSSION

From CHAPTER 1 to CHAPTER 2, the author have demonstrated that the major phosphorylation sites of N protein (S479 and S510) were involved in various stages of the viral lifecycle (Sugai, *et al*., 2012; Sugai, *et al*., 2013). Additionally, it has been shown that a double mutant of the major phosphorylation sites remained phosphorylated but to a lesser extent, suggesting unidentified phosphorylation sites within the N protein existed. In this chapter, nine putative minor phosphorylation sites of N protein were predicted by MS analysis. Moreover, the author demonstrated that a threonine residue at location 279 was notably phosphorylated among the putative minor phosphorylation sites and was a prerequisite for NC formation.

Since the late 1970s, it has been known that N protein undergoes phosphorylation at both serine and threonine residues, and that the phosphorylation intensity of phosphoserine was stronger than for phosphothreonine (Robbins, *et al*., 1980; Robbins and Bussell, 1979). Additionally, in the 1990s, it was reported that the phosphorylation intensity of phosphoserine and phosphothreonine was 88% and 12%, respectively, of the total N-phosphorylation (Gombart, *et al*., 1995). In agreement with these reports, the author demonstrated that the phosphorylation intensity of a double mutant of the major phosphorylation sites (S479A/S510A) was 15.7% compared to wt-N protein, and the phosphorylation intensity of the T279 site was 14.3% of the total N-phosphorylation. This indicated that the intensity of major phosphorylation at serine residues was 84.3%, and almost all of the remaining 15.7% phosphorylation was due to

phosphorylation of T279. Furthermore, specific phosphorylation was not detected in the ST11A mutant (Fig. 2E and F), suggesting no significant phosphorylation sites other than the 11 sites already identified. In addition, alanine substitution at putative minor phosphorylation sites other than T279 did not have influence in a minigenome expression assay. Taken together, these data indicated that the functionally significant phosphorylation sites of N protein were limited to the two major phosphorylation sites (S479 and S510) and a minor T279 phosphorylation site.

It was reported that free N protein and NC-associated N protein showed different antigenicity toward antibodies, and was explained as a conformational difference between the free N protein and NC-associated N protein (Kawai, *et al*., 1999; Gombert, *et al*., 1993; Hirano, *et al*., 1992). This suggested that conformational changes of N protein were required for NC formation. Furthermore, free N protein is phosphorylated only on serine residues, whereas the NC-associated N protein is phosphorylated on both serine and threonine residues (Gombart, *et al*., 1995), implying that threonine phosphorylation and subsequent conformational changes of N protein are a prerequisite to NC formation. In agreement with these studies, the author demonstrated that the T279A mutant did not form NC-like particles by electron microscopy. Additionally, the data also suggested that an absence of phosphorylation at the threonine residue resulted in a structural abnormality in the NC-like particle. Taken together, these data indicated that NC formation requires a conformational change of N protein that is switched by phosphorylation at T279. However, wt-N protein and T279A mutant harvested from NC fractions of CsCl density gradients did not show any

difference in proteolytic peptide patterns of trypsin digestion, indicating that the T279A mutant retained a normal tertiary structure similar to the wt-N protein. Thus, the conformational change required for NC formation was a quite small and cannot be discriminated from trypsin digestion patterns. Indeed, trypsin digestion of free N protein and NC-associated N protein resulted in similar degradation patterns (Gombart, *et al*., 1995). Moreover, a double mutant of the MV-N CCR domain whose SL (residues 228-229) were replaced by QD (NQD) did not cause any differences in trypsin digestion analysis, immunoprecipitation, and circular dichroism (CD) spectroscopy, while the mutant did not form normal NC-like particles by electron microscopy (Karlin, *et al*., 2002). As the conformational change for NC formation could not be detected by CD spectroscopy, the change was not accompanied by a change in secondary structure. Thus, in the NC formation step, very small conformational changes are required for correct encapsidation.

Since the CsCl gradient centrifugation assay suggested that the ST10A mutant formed normal NC-like particles, the major phosphorylation sites of N protein are dispensable for NC formation. This is consistent with a previous report demonstrating the N-tail region is not required for NC formation (Buchholz, *et al*., 1993). Here, we identified the T279 site as a new phosphate group acceptor site that is indispensable for NC formation. However, the phosphorylation intensity of T279 was low, and this minor phosphorylation was only 14.3% of the total N-phosphorylation. Moreover, substitution of T279 to acidic residues such as aspartic acid and glutamic acid also abrogated the phenotype of wt-N protein in a minigenome assay and in IFA. Thus, the

phosphorylation at T279 is not constitutive, and N protein is functionally inactive under circumstances where all N proteins are constantly phosphorylated at T279. Moreover, although the threonine residue of free N protein was not phosphorylated (Gombart, *et al*., 1995), 14.3% of the NC-associated N proteins were phosphorylated at T279. This indicates that one seventh of the NC-associated N proteins are phosphorylated when N proteins incorporate into the nascent N-RNA complex. Whether N proteins are expressed by plasmid or during viral replication (Gombart, *et al*., 1995), the phosphorylation rate of the threonine residue in NC was almost at the same level. Thus, T279 phosphorylation of the N protein is required for the maintenance of the herringbone-like structure of NC, and is different from the major phosphorylation sites that take part in the functional regulation of viral gene expression (Hagiwara, *et al*., 2008; Sugai, *et al*., 2012; Sugai, *et al*., 2013). Electron microscopy demonstrated that NC has a helical structure with approximately 13-14 N proteins per turn (Bhella, *et al*., 2004; Kolakofsky, *et al*., 2005; Bhella, *et al*., 2002). Therefore, N proteins may change its own conformation through the phosphorylation of T279 at a ratio of 1 per 7 to cancel the structural distortion of the NC.

In the present study, the author demonstrated that phosphorylation at T279 is a prerequisite for NC formation. However, the relationship between T279 phosphorylation and conformational changes of NC-associated N proteins remain to be clarified. Further analysis of the conformational change in N protein might reveal the precise mechanism of NC formation.

FIGURE LEGENDS

Fig. 1

Identification of the minor phosphorylation sites in the N protein by MS analysis. (A) Trypsin-digested peptides of N protein were separated by nanoflow-LC and analyzed by MALDI-TOF/TOF MS. (B) Phosphorylated peptides from V8 protease-digested N proteins were selectively analyzed and identified by MALDI-TOF/TOF MS. The analyzed peptides were identified with MASCOT ver. 2.0 database search and are shown in red.

Fig. 2

Analysis of minor phosphorylation sites of N protein. (A) Schematic diagram of the alanine substitution mutants of the N protein used in this study. Each phosphorylation site is indicated as a green square, and sites substituted with alanine residues are shown as a red square with an initial-letter "A". (B) Identification of the minor phosphorylation site in the N protein by immunoprecipitation assay. The N protein or its phosphorylation mutants were radio-labeled with ^{32}P or ^{35}S in Cos7 cells. Relative phosphorylation (^{32}P-N/^{35}S-N) of each N protein mutant was quantified. (C) Phosphorylation of wt-N and the T279A mutant in 293T and Vero cells.

Fig. 3 Phosphorylation analysis of the other serine and threonine residues within N protein. (A) Multiple sequence alignment of the N protein CCR (aa 258-357) from

Paramyxoviruses: canine distemper virus (GenBank Accession No. AAG30916), rinderpest virus (CAA48388), peste des petits ruminants virus (ACN62116), Hendra virus (AAC83187), Nipah virus (AAK50548), Sendai virus (AAB06278), mumps virus (CBA10117), and human parainfluenza virus type 1 (NP_604433). Black and red arrowheads indicate untested S or T residues by MS analysis and putative phosphorylation sites detected by MS analysis, respectively. (B) Schematic diagram of additional mutants at the CCR, and (C) phosphorylation properties of the mutants.

Fig. 4

Functional analysis of minor phosphorylation sites. (A) Minigenome assay using alanine substitution mutants of the N protein. 293 cells were transfected with minigenomic RNA and plasmids for the N, P, and L proteins. On the following day, luciferase activity of the cell lysates was measured. (B) Minigenome assay using N protein mutants whose T279 site was replaced by acidic residues.

Fig. 5

Localization and N-P binding ability of T279A mutant. (A) T279 mutants showed diffuse cytoplasmic distribution. Cos7 cells were transfected with the plasmid expressing the wt-N or T279A mutants, and the localization of each protein was detected with anti-N polyclonal antibody. (B) Localization of other N protein mutants, and (C) distribution of wt-N and T279A mutant in the presence of the P protein were evaluated. (D) The wt-N or T279A mutant was transfected into Cos7 cells, along with

the P protein. Proteins were labeled with ^{35}S and co-precipitated with the anti-N polyclonal antibody. The bar graph shows the relative quantity of P protein coprecipitated with N protein (P protein/N protein). Error bars indicate standard deviation.

Fig. 6

The T279A mutant of the N protein failed to form NC-like particles. (A) Cos7 cells were transfected with wt-N or T279A plasmids, and N protein expression levels in cell lysates and NC fractions of CsCl density gradient centrifugation are shown. Bar graphs indicate the relative expression levels of N protein. Error bars indicate standard deviation. (B) Electron microscopy of wt-N and T279A in the NC fraction of CsCl density gradient centrifugation. Bar represents 50 nm.

Fig. 7

The T279A mutant showed the same proteolytic pattern as the wt-N protein. The wt-N, T279A, and heat-denatured wt-N proteins were treated with various concentrations of trypsin. High contrasted image of the low molecular weight region (<37 kDa) is shown for low-density degradation products. Arrowheads indicate the various degradation products of the denatured N protein.

Fig. 8

Dephosphorylation of T279 by BAP treatment impairs NC formation. NC-like particles

of the wt-N or N protein mutants were separated by CsCl gradient centrifugation. Gradients were divided into 7 fractions, and N protein in each fraction was detected. (A) wt-N, (B) T279A, (C) ST10A, (D) ST10A with BAP treatment, and (E) ST10A with BAP and phosphatase inhibitor. Bar graphs show the percentage of N protein content in each fraction per total N protein in the 7 fractions.

A

Trypsin treatment

```
  1 MATLLRSLAL FKRNKDKPPI TSGSGGAIRG IKHIIIVPIP GDSSITTRSR
 51 LLDRLVRLIG NPDVSGPKLT GALIGILSLF VESPGQLIQR ITDDPDVSIR
101 LLEVVQSDQS QSGLTFASRG TNMEDEADQY FSHDDPSNSD QSRSGWFENK
151 EISDIEVQDP EGFNMILGTI LAQIWVLLAK AVTAPDTAAD SELRRWIKYT
201 QQRRVVGEFR LERKWLDVVR NRIAEDLSLR RFMVALILDI KRTPGNKPRI
251 AEMICDIDTY IVEAGLASFI LTIKFGIETM YPALGLHEFA GELSTLESLM
301 NLYQQMGETA PYMVILENSI QNKFSAGSYP LLWSYAMGVG VELENSMGGL
351 NFGRSYFDPA YFRLGQEMVR RSAGKVSSTL ASELGITAED ARLVSEIAMH
401 TTEDRISRAV GPRQAQVSFL HGDQSENELP GLGGKEDRRV KQGRGEAREN
451 YRETGSSRAS DARAAHPPTS MPLDIDTASE SGQDPQDSQR SADALLRLQA
501 MAGILEEQGS DTDTPRVYND RDLLD
```

B

V8 protease treatment

```
  1 MATLLRSLAL FKRNKDKPPI TSGSGGAIRG IKHIIIVPIP GDSSITTRSR
 51 LLDRLVRLIG NPDVSGPKLT GALIGILSLF VESPGQLIQR ITDDPDVSIR
101 LLEVVQSDQS QSGLTFASRG TNMEDEADQY FSHDDPSNSD QSRSGWFENK
151 EISDIEVQDP EGFNMILGTI LAQIWVLLAK AVTAPDTAAD SELRRWIKYT
201 QQRRVVGEFR LERKWLDVVR NRIAEDLSLR RFMVALILDI KRTPGNKPRI
251 AEMICDIDTY IVEAGLASFI LTIKFGIETM YPALGLHEFA GELSTLESLM
301 NLYQQMGETA PYMVILENSI QNKFSAGSYP LLWSYAMGVG VELENSMGGL
351 NFGRSYFDPA YFRLGQEMVR RSAGKVSSTL ASELGITAED ARLVSEIAMH
401 TTEDRISRAV GPRQAQVSFL HGDQSENELP GLGGKEDRRV KQGRGEAREN
451 YRETGSSRAS DARAAHPPTS MPLDIDTASE SGQDPQDSQR SADALLRLQA
501 MAGILEEQGS DTDTPRVYND RDLLD
```

Chapter 3 - Figure 1

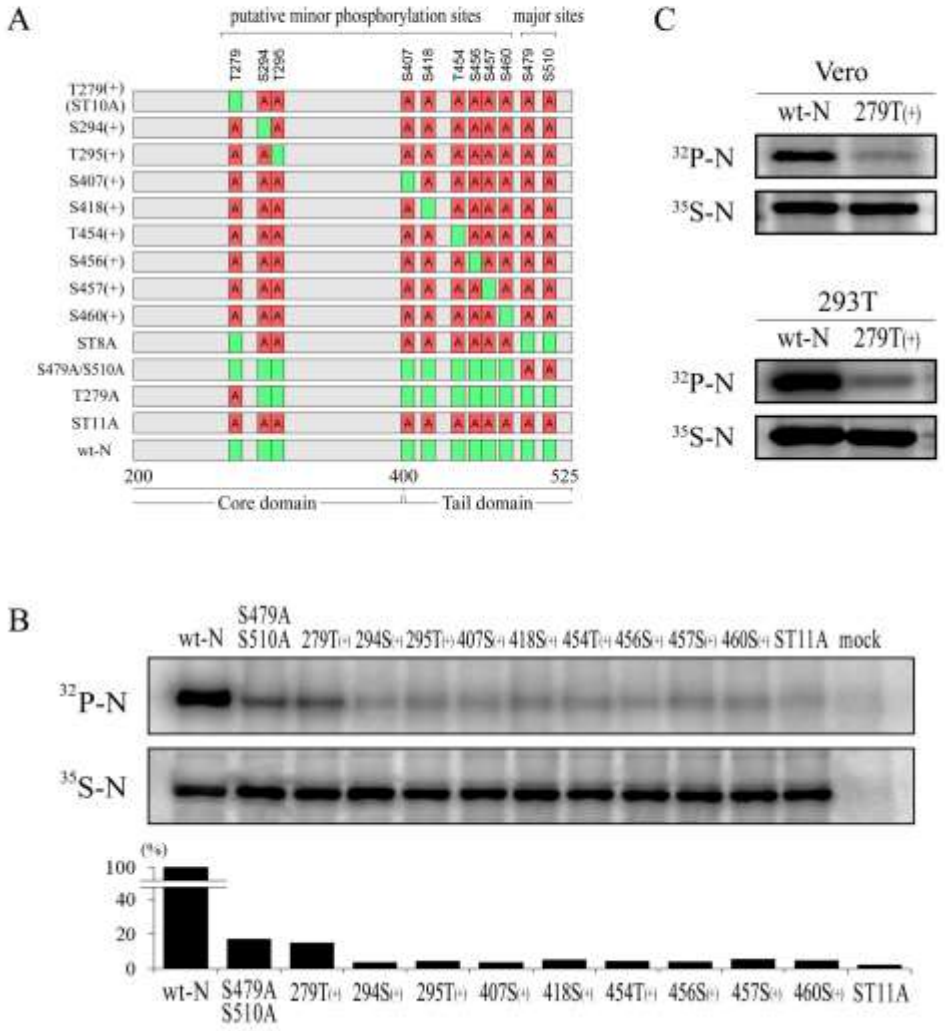

Chapter 3 - Figure 2

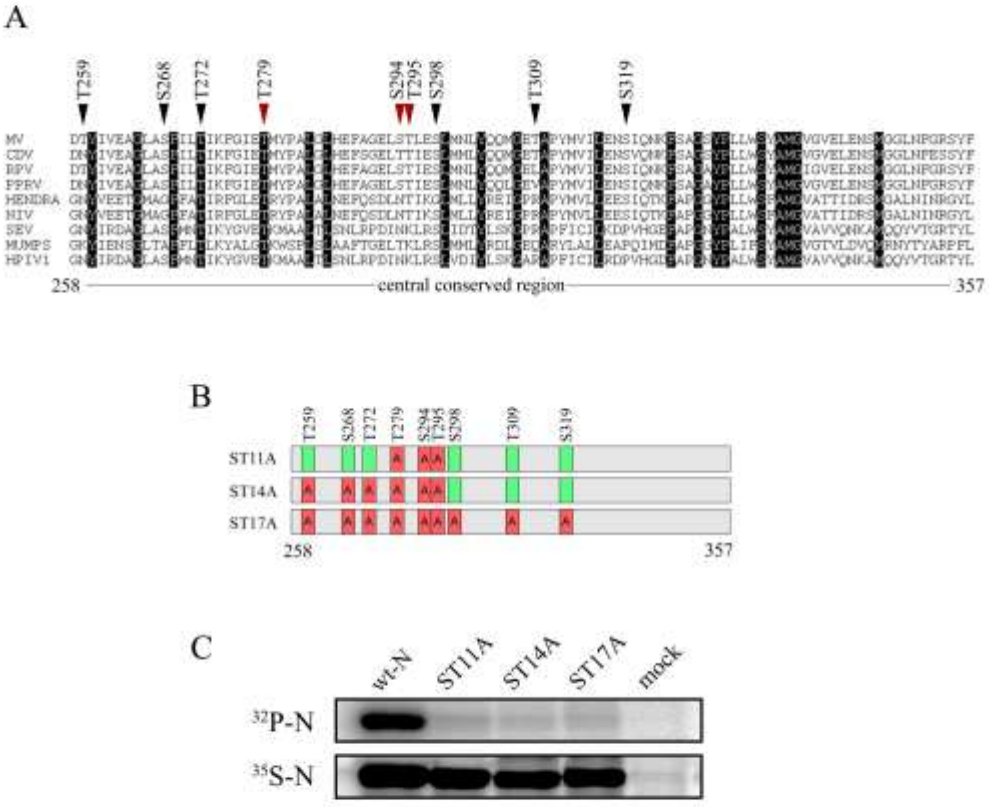

Chapter 3 - Figure 3

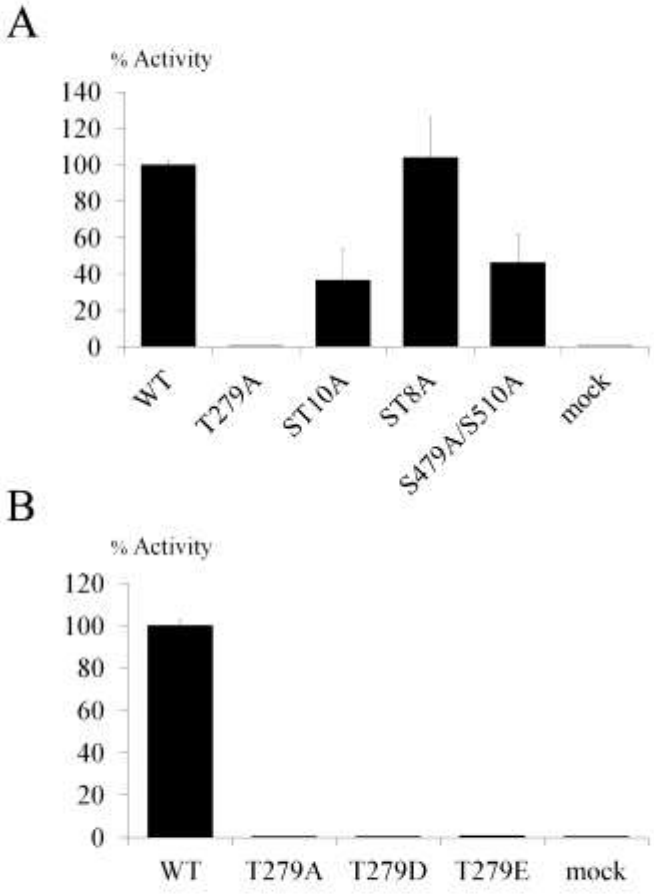

Chapter 3 - Figure 4

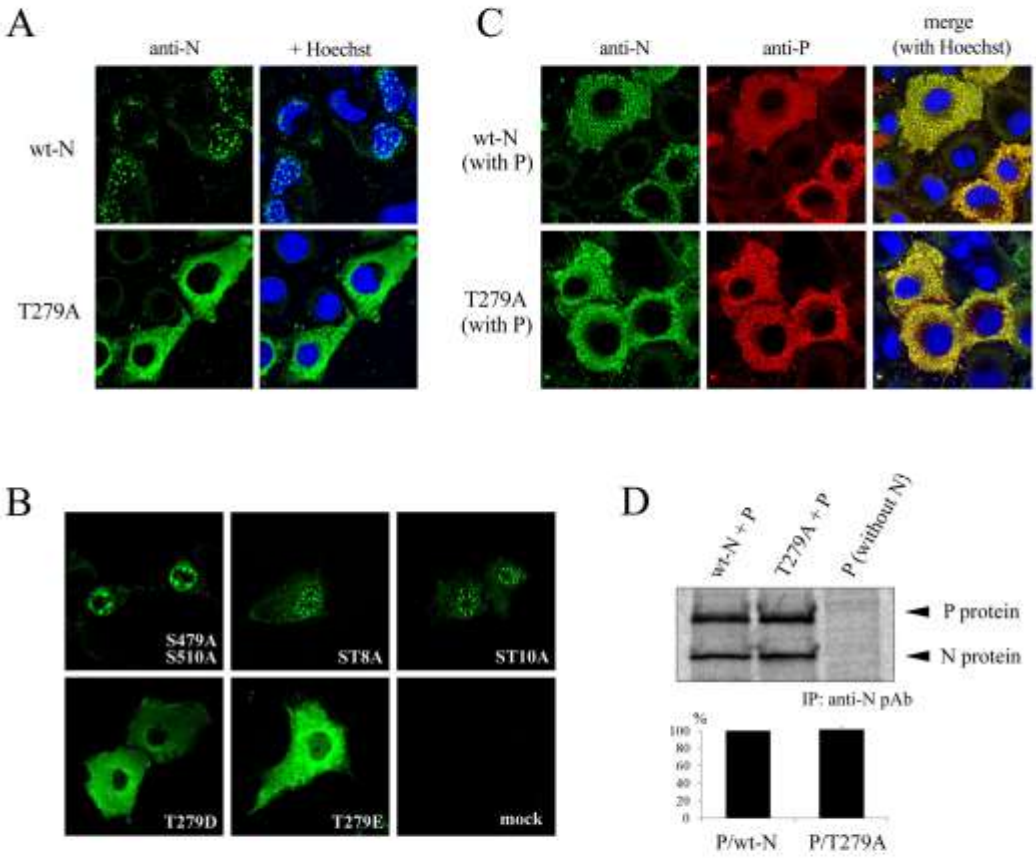

Chapter 3 - Figure 5

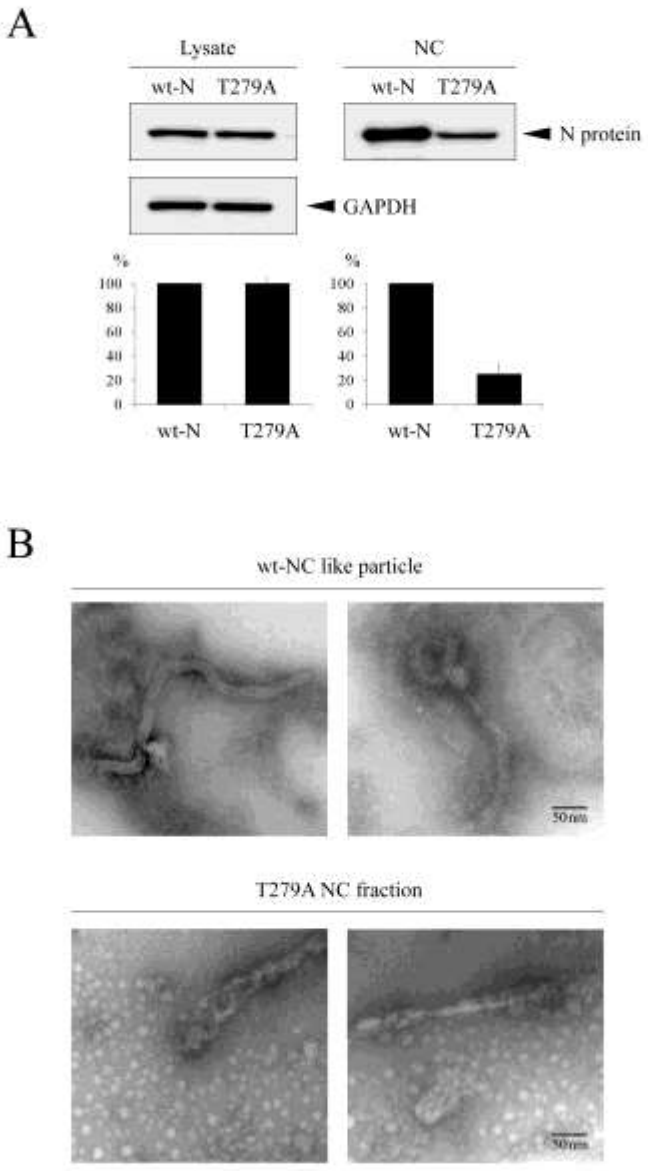

Chapter 3 - Figure 6

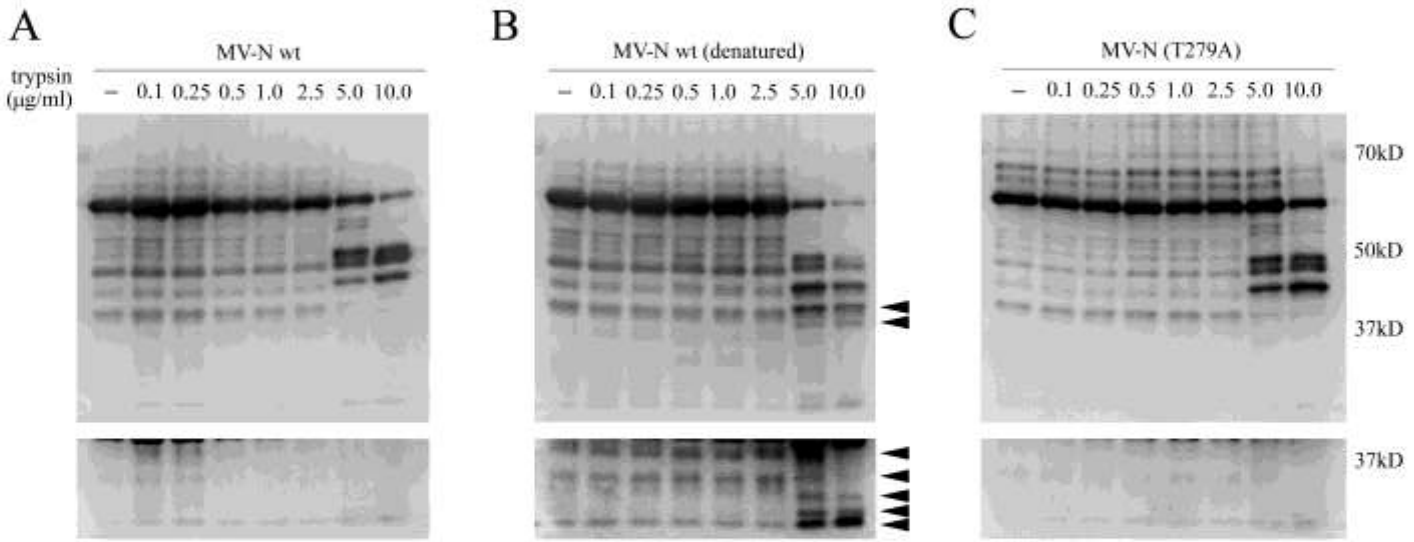

Chapter 3 - Figure 7

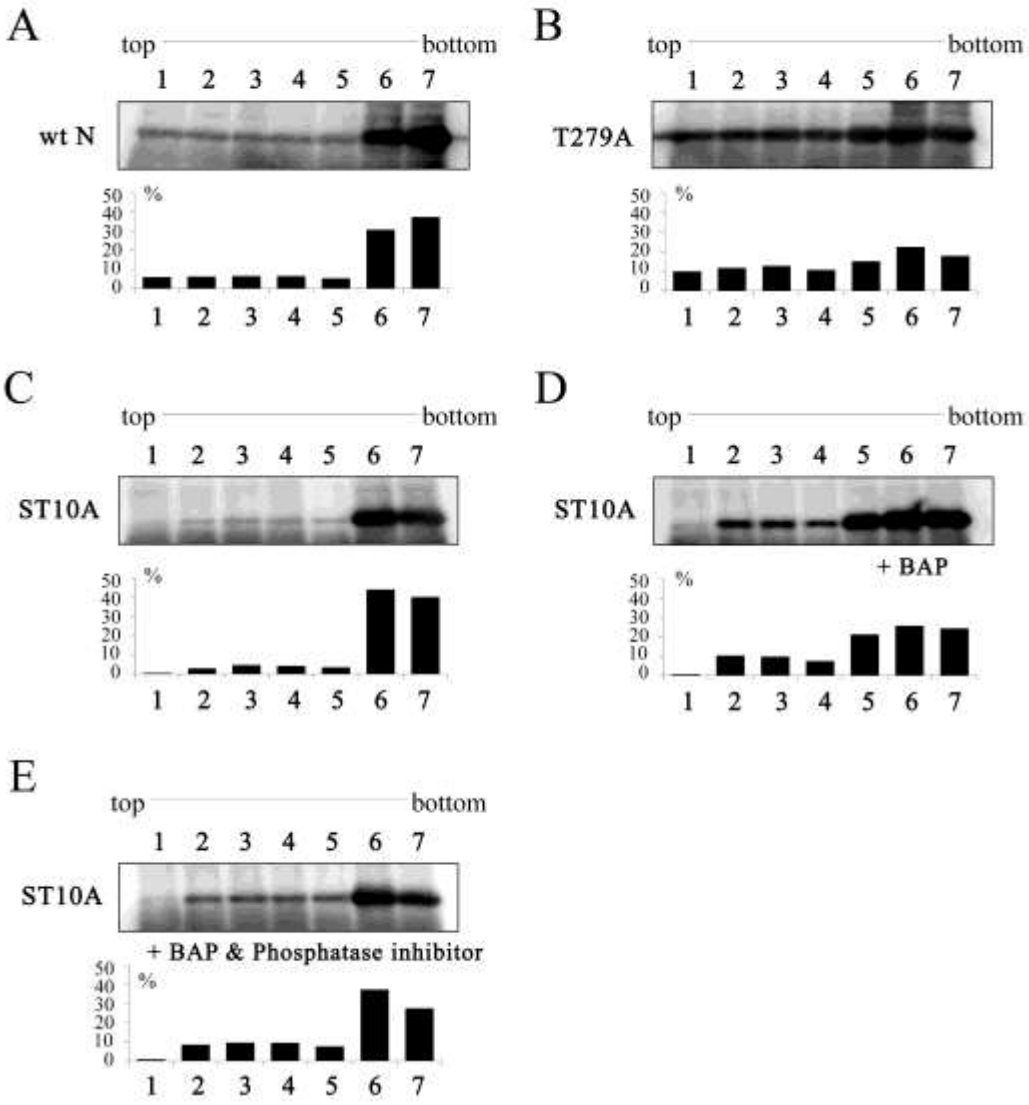

Chapter 3 - Figure 8

CONCLUDING REMARKS

In this study, detailed analyses of phosphorylation sites within measles virus N and P proteins were conducted. The author identified some phosphorylation sites, and investigated the functions of the phosphorylations.

In CHAPTER1, the author reported a significant inverse correlation between the phosphorylation level of MV-P protein and viral transcriptional activity. Upregulation of P protein phosphorylation resulted in reduction of viral transcription. Additionally, the author demonstrated that the strong phosphorylation at S86 and S151 of P protein, which may be generally regulated by association with nucleoprotein, downregulates the viral transcriptional activity. Taken together, these findings suggest that P protein is involved in the regulation of viral transcription by altering its own phosphorylation property.

In CHAPTER2, to investigate the functional significance of N protein phosphorylation, the author rescued recombinant MVs (rMVs) whose phosphorylation sites of N protein were substituted with alanine residue (rMV-S479A, rMV-S510A, and rMV-S479A/S510A) using a reverse genetics system, and analyses of these recombinants were conducted. In the single-step growth experiment, rMVs showed more rapid growth kinetics and N protein accumulation than those of wild type MV. It has been also demonstrated that the enhancement of viral gene expression was accompanied by high levels of cytokine induction. These suggested that N-phosphorylation had an important role to control the viral growth rate through regulating viral gene expression during the early phase of rMV infection. On the other

hand, the multi-step growth curves revealed that N-phosphorylation intensity correlated inversely with virus yield. Moreover, excessive N-phosphorylation resulted in the lower stability against RNase and the faster turnover of the viral genome RNA. Taken together, these results suggest that N-phosphorylation is involved in both the viral gene expression and viral genome RNA stability.

In CHAPTER3, the author identified new phosphorylation site of measles virus N protein, and analyzed the function of the phosphorylation. Using mass spectrometry, nine putative phosphorylation sites within N protein were identified. The author generated alanine substitution mutants for each putative phosphorylation site of N protein and examined the phosphorylation signals by ^{32}P labeling. Among these nine putative phosphorylation sites, the T279 site was remarkably phosphorylated. The eight putative phosphorylation sites other than T279 were not required for N-protein function in the minigenome expression assays, but the T279 site was functionally essential. Limited proteolysis and electron microscopy showed that a T279A mutant was not denatured but lacked the ability for nucleocapsid assembly. Furthermore, dephosphorylation treatment of the T279 site by alkaline phosphatase caused deficiencies in nucleocapsid formation. Taken together, these results indicate that phosphorylation at T279 of N protein is indispensable for functional nucleocapsid formation.

Thus, in this study, the author have demonstrated that the phosphorylation of N and P proteins involved in the various steps of viral life cycles such as regulation of viral transcriptional activity, viral gene expression level, viral genome stability, and

nucleocapsid formation. This is the first report investigating the functions of phosphorylation modifications of MV structural proteins using recombinant viruses. These findings would shed light on the functional significance of viral protein phosphorylation in viral life cycle.

REFERENCES

Akramuzzaman SM, Cutts FT, Wheeler JG, Hossain MJ. 2000. Increased childhood morbidity after measles is short-term in urban Bangladesh. Am J Epidemiol. 151(7):723-35.

Appel, M. J., R. A. Yates, G. L. Foley, J. J. Bernstein, S. Santinelli, L. H. Spelman, L. D. Miller, L. H. Arp, M. Anderson, M. Barr, S. Pearce-Kelling, and B. A. Summers. 1994. Canine distemper epizootic in lions, tigers, and leopards in North America. J. Vet. Diagn. Investig. 6:277–288

Asenjo A, González-Armas JC, Villanueva N. 2008. Phosphorylation of human respiratory syncytial virus P protein at serine 54 regulates viral uncoating. Virology. 380(1):26-33.

Asenjo A, Rodríguez L, Villanueva N. 2005. Determination of phosphorylated residues from human respiratory syncytial virus P protein that are dynamically dephosphorylated by cellular phosphatases: a possible role for serine 54. J Gen Virol. 86(Pt 4):1109-20.

Barik S, McLean T, Dupuy LC. 1995. Phosphorylation of Ser232 directly regulates the transcriptional activity of the P protein of human respiratory syncytial virus: phosphorylation of Ser237 may play an accessory role. Virology. 213(2):405–412

Baron MD, Barrett T. 1997. Rescue of rinderpest virus from cloned cDNA. J. Virol. 71(2):1265–1271

Beckford, A. P., R. O. C. Kaschula, and C. Stephen. 1985. Factors associated with fatal cases of measles: a retrospective autopsy study. S. Afr. Med. J. 68:858–863.

Bellini WJ, Englund G, Rozenblatt S, Arnheiter H, Richardson CD. 1985. Measles virus P gene codes for two proteins. J. Virol. 53(3):908–919

Bernard C, Gely S, Bourhis JM, Morelli X, Longhi S, Darbon H. 2009. Interaction between the C-terminal domains of N and P proteins of measles virus investigated by NMR. FEBS Lett.

583(7):1084-9.

Bhella D, Ralph A, Murphy LB, Yeo RP. 2002. Significant differences in nucleocapsid morphology within the Paramyxoviridae. J Gen Virol. 83:1831-9.

Bhella D, Ralph A, Yeo RP. 2004. Conformational flexibility in recombinant measles virus nucleocapsids visualised by cryo-negative stain electron microscopy and real-space helical reconstruction. J Mol Biol. 340(2):319-31.

Bitko V, Barik S. 2001. Phenotypic silencing of cytoplasmic genes using sequence-specific double-stranded short interfering RNA and its application in the reverse genetics of wild type negative-strand RNA viruses. BMC Microbiol. 1:34.

Bourhis JM, Receveur-Bréchot V, Oglesbee M, Zhang X, Buccellato M, Darbon H, Canard B, Finet S, Longhi S. 2005. The intrinsically disordered C-terminal domain of the measles virus nucleoprotein interacts with the C-terminal domain of the phosphoprotein via two distinct sites and remains predominantly unfolded. Protein Sci. 14:1975-92.

Brown DD, Collins FM, Duprex WP, Baron MD. 2005. 'Rescue' of mini-genomic constructs and viruses by combinations of morbillivirus N, P and L proteins. J. Gen. Virol. 86:1077–1081

Bryce J, Boschi-Pinto C, Shibuya K, Black RE; WHO Child Health Epidemiology Reference Group. 2005. WHO estimates of the causes of death in children. Lancet. 365(9465):1147-52.

Buchholz CJ, Spehner D, Drillien R, Neubert WJ, Homann HE. 1993. The conserved N-terminal region of Sendai virus nucleocapsid protein NP is required for nucleocapsid assembly. J Virol. 67:5803-12.

Calain P, Roux L. 1993. The rule of six, a basic feature for efficient replication of Sendai virus defective interfering RNA. J Virol. 67(8):4822-30.

Cattaneo R, Kaelin K, Baczko K, Billeter MA. 1989. Measles virus editing provides an

additional cysteine-rich protein. Cell. 56(5):759–764

Centers for Disease Control and Prevention (CDC). 2008. Progress in global measles control and mortality reduction, 2000-2007. MMWR Morb Mortal Wkly Rep. 57:1303-6.

Centers for Disease Control and Prevention (CDC). 2013. Global control and regional elimination of measles, 2000-2011. MMWR Morb Mortal Wkly Rep. 18;62(2):27-31.

Cevik B, Holmes DE, Vrotsos E, Feller JA, Smallwood S, Moyer SA. 2004. The phosphoprotein (P) and L binding sites reside in the N-terminus of the L subunit of the measles virus RNA polymerase. Virology. 327(2):297-306.

Curran J. 1996. Reexamination of the Sendai virus P protein domains required for RNA synthesis: a possible supplemental role for the P protein. Virology. 221(1):130-40.

Das T, Schuster A, Schneider-Schaulies S, Banerjee AK. 1995. Involvement of cellular casein kinase II in the phosphorylation of measles virus P protein: identification of phosphorylation sites. Virology. 211(1):218–226

De BP, Gupta S, Gupta S, Banerjee AK. 1995. Cellular protein kinase C isoform zeta regulates human parainfluenza virus type 3 replication. Proc. Natl. Acad. Sci. USA. 92(11):5204–5208

de Vries RD, McQuaid S, van Amerongen G, Yuksel S, Verburgh RJ, Osterhaus AD, Duprex WP, de Swart RL. 2012. Measles immune sup- pression: lessons from the macaque model. PLoS Pathog. 8:e1002885.

Delpeut S, Noyce RS, Richardson CD. 2014. The tumor-associated marker, PVRL4 (nectin-4), is the epithelial receptor for morbilliviruses. Viruses. 6(6):2268-86.

Dhiman N, Jacobson RM, Poland GA. 2004. Measles virus receptors: SLAM and CD46. Rev Med Virol. 14(4):217-29.

Dillon, P. J., and G. D. Parks. 2007. A role for the P subunit of the paramyxovirus polymerase in limiting host cell antiviral responses. J. Virol. 81(20):11116-27.

Dörig RE, Marcil A, Richardson CD. 1994. CD46, a primate-specific receptor for measles virus. Trends Microbiol. 2(9):312-8.

Dowling PC, Blumberg BM, Menonna J, Adamus JE, Cook P, Crowley JC. 1986. Transcriptional map of the measles virus genome. J. Gen. Virol. 1987–1992

Fooks AR, Stephenson JR, Warnes A, Dowsett AB, Rima BK, Wilkinson GW. 1993. Measles virus nucleocapsid protein expressed in insect cells assembles into nucleocapsid-like structures. J Gen Virol. 74:1439-44.

Fuentes SM, Sun D, Schmitt AP, He B. 2010. Phosphorylation of paramyxovirus phosphoprotein and its role in viral gene expression. Future Microbiol. 5(1):9-13

Gainey MD, Dillon PJ, Clark KM, Manuse MJ, Parks GD. 2008. Paramyxovirus-induced shutoff of host and viral protein synthesis: role of the P and V proteins in limiting PKR activation. J Virol. 82(2):828-39.

Gao Y, Lenard J. 1995. Multimerization and transcriptional activation of the phosphoprotein (P) of vesicular stomatitis virus by casein kinase-II. EMBO J. 14(6):1240–1247

Gely S, Lowry DF, Bernard C, Jensen MR, Blackledge M, Costanzo S, Bourhis JM, Darbon H, Daughdrill G, Longhi S. 2010. Solution structure of the C-terminal X domain of the measles virus phosphoprotein and interaction with the intrinsically disordered C-terminal domain of the nucleoprotein. J Mol Recognit. 23:435-447.

Gemma T, Watari T, Akiyama K, Miyashita N, Shin YS, Iwatsuki K, Kai C, Mikami T. 1996. Epidemiological observations on recent outbreaks of canine distemper in Tokyo area. J Vet Med Sci. 58(6):547-50.

Gluzman Y. 1981. SV40-transformed simian cells support the replication of early SV40 mutants. Cell. 23(1):175–182

Gombart AF, Hirano A, Wong TC. 1993. Conformational maturation of measles virus nucleocapsid protein. J Virol. 67:4133-41.

Gombart AF, Hirano A, Wong TC. 1995. Nucleoprotein phosphorylated on both serine and threonine is preferentially assembled into the nucleocapsids of measles virus. Virus Res. 37:63-73.

Hagiwara K, Sato H, Inoue Y, Watanabe A, Yoneda M, Ikeda F, Fujita K, Fukuda H, Takamura C, Kozuka-Hata H, Oyama M, Sugano S, Ohmi S, Kai C. 2008. Phosphorylation of measles virus nucleoprotein upregulates the transcriptional activity of minigenomic RNA. Proteomics. 8(9):1871-9.

Harrison MS, Sakaguchi T, Schmitt AP. 2010. Paramyxovirus assembly and budding: building particles that transmit infections. Int J Biochem Cell Biol. 42(9):1416-29.

Hashiguchi T, Maenaka K, Yanagi Y. 2011. Measles virus hemagglutinin: structural insights into cell entry and measles vaccine. Front Microbiol. 2-247..

Heggeness MH, Scheid A, Choppin PW. 1981. The relationship of conformational changes in the Sendai virus nucleocapsid to proteolytic cleavage of the NP polypeptide. Virology. 114:555-62.

Hirano A, Wang AH, Gombart AF, Wong TC. 1992. The matrix proteins of neurovirulent subacute sclerosing panencephalitis virus and its acute measles virus progenitor are functionally different. Proc Natl Acad Sci U S A. 89:8745-9.

Houben K, Marion D, Tarbouriech N, Ruigrok RW, Blanchard L. 2007. Interaction of the C-terminal domains of sendai virus N and P proteins: comparison of polymerase-nucleocapsid interactions within the paramyxovirus family. J. Virol. 81(13):6807–6816.

Howie D, Simarro M, Sayos J, Guirado M, Sancho J, Terhorst C. 2002. Molecular dissection of the signaling and costimulatory functions of CD150 (SLAM): CD150/SAP binding and CD150-mediated costimulation. Blood. 99(3):957-65.

Huang M, Sato H, Hagiwara K, Watanabe A, Sugai A, Ikeda F, Kozuka-Hata H, Oyama M, Yoneda M, Kai C. 2011. Determination of a phosphorylation site in Nipah virus nucleoprotein and its involvement in virus transcription. J Gen Virol. 92:2133-41.

Huber M, Cattaneo R, Spielhofer P, Orvell C, Norrby E, Messerli M, Perriard JC, Billeter MA. 1991. Measles virus phosphoprotein retains the nucleocapsid protein in the cytoplasm. Virology. 185(1):299-308.

Huntley CC, De BP, Banerjee AK. 1997. Phosphorylation of sendai virus phosphoprotein by cellular protein kinase C zeta. J. Biol. Chem. 272(26):16578–16584

Huntley CC, De BP, Murray NR, Fields AP, Banerjee AK. 1995. Human parainfluenza virus type 3 phosphoprotein: identification of serine 333 as the major site for PKC zeta phosphorylation. Virology. 211(2):561–567

Hussey GD, Clements CJ. 1996. Clinical problems in measles case management. Ann Trop Paediatr 16: 307–317.

Iwasaki M, Takeda M, Shirogane Y, Nakatsu Y, Nakamura T, Yanagi Y. 2009. The matrix protein of measles virus regulates viral RNA synthesis and assembly by interacting with the nucleocapsid protein. J Virol. 83(20):10374-83.

Kai C, Ochikubo F, Okita M, Iinuma T, Mikami T, Kobune F, Yamanouchi K. 1993. Use of B95a cells for isolation of canine distemper virus from clinical cases. J Vet Med Sci. 55(6):1067-70.

Karlin D, Ferron F, Canard B, Longhi S. 2003. Structural disorder and modular organization in Paramyxovirinae N and P. J Gen Virol. 84(Pt 12):3239-52.

Karlin D, Longhi S, Canard B. 2002. Substitution of two residues in the measles virus nucleoprotein results in an impaired self-association. Virology. 302:420-32.

Kaushik R, Shaila MS. 2004. Cellular casein kinase II-mediated phosphorylation of rinderpest virus P protein is a prerequisite for its role in replication/transcription of the genome. J. Gen. Virol. 85(Pt 3):687–691

Kawai A, Toriumi H, Tochikura TS, Takahashi T, Honda Y, Morimoto K. 1999. Nucleocapsid formation and/or subsequent conformational change of rabies virus nucleoprotein (N) is a prerequisite step for acquiring the phosphatase-sensitive epitope of monoclonal antibody 5-2-26. Virology. 263(2):395-407.

Kitchen J, Saunders RE, Warwicker J. 2008. Charge environments around phosphorylation sites in proteins. BMC Struct Biol. 8:19.

Kobune F, Sakata H, Sugiura A. 1990. Marmoset lymphoblastoid cells as a sensitive host for isolation of measles virus. J Virol. 64(2):700-5.

Kobune F, Takahashi H, Terao K, Ohkawa T, Ami Y, Suzaki Y, Nagata N, Sakata H, Yamanouchi K, Kai C. 1996. Nonhuman primate models of measles. Lab Anim Sci. 46(3):315-20.

Kolakofsky D, Le Mercier P, Iseni F, Garcin D. 2004. Viral DNA polymerase scanning and the gymnastics of Sendai virus RNA synthesis. Virology. 318(2):463-73.

Kolakofsky D, Roux L, Garcin D, Ruigrok RW. 2005. Paramyxovirus mRNA editing, the "rule of six" and error catastrophe: a hypothesis. J Gen Virol. 86:1869-77.

Kujime K, Hashimoto S, Gon Y, Shimizu K, Horie T. 2000. p38 mitogen-activated protein kinase and c-jun-NH2-terminal kinase regulate RANTES production by influenza virus-infected human bronchial epithelial cells. J Immunol. 164(6):3222-8.

References

Leyrat C, Yabukarski F, Tarbouriech N, Ribeiro EA Jr, Jensen MR, Blackledge M, Ruigrok RW, Jamin M. 2011. Structure of the vesicular stomatitis virus N^0 -P complex. PLoS Pathog. 7(9):e1002248.

Liston P, Batal R, DiFlumeri C, Briedis DJ. 1997. Protein interaction domains of the measles virus nucleocapsid protein (NP). Arch Virol. 142:305-21.

Liu Z, Huntley CC, De BP, Das T, Banerjee AK, Oglesbee MJ. 1997. Phosphorylation of canine distemper virus P protein by protein kinase C-zeta and casein kinase II. Virology. 232(1):198–206

Longhi S, Receveur-Bréchot V, Karlin D, Johansson K, Darbon H, Bhella D. 2003. The C-terminal domain of the measles virus nucleoprotein is intrinsically disordered and folds upon binding to the C-terminal moiety of the phosphoprotein. J. Biol. Chem. 278(20):18638–18648

Lu B, Ma CH, Brazas R, Jin H. 2002. The major phosphorylation sites of the respiratory syncytial virus phosphoprotein are dispensable for virus replication in vitro. J Virol. 76(21):10776-84.

Lund GA, Tyrrell DL, Bradley RD, Scraba DG. 1984. The molecular length of measles virus RNA and the structural organization of measles nucleocapsids. J Gen Virol. 65 (Pt 9):1535-42.

Masuda M, Sato H, Kamata H, Katsuo T, Takenaka A, Miura R, Yoneda M, Tsukiyama-Kohara K, Mizumoto K, Kai C. 2006. Characterization of monoclonal antibodies directed against the canine distemper virus nucleocapsid protein. Comp Immunol Microbiol Infect Dis. 29(2-3): 157-65.

McLeod WJ. 1964. Measles Vaccine .Br Med J. 2(5418): 1197.

Moyer SA, Baker SC, Horikami SM. 1990. Host cell proteins required for measles virus reproduction. J Gen Virol. 71:775-83.

Moyer SA, Smallwood-Kentro S, Haddad A, Prevec L. 1991. Assembly and transcription of synthetic vesicular stomatitis virus nucleocapsids. J Virol. 65(5):2170-8.

Mühlebach MD, Mateo M, Sinn PL, Prüfer S, Uhlig KM, Leonard VH, Navaratnarajah CK, Frenzke M, Wong XX, Sawatsky B, Ramachandran S, McCray PB Jr, Cichutek K, von Messling V, Lopez M, Cattaneo R. 2011. Adherens junction protein nectin-4 is the epithelial receptor for measles virus. Nature. 480(7378):530-3.

Myers TM, Pieters A, Moyer SA. 1997. A highly conserved region of the Sendai virus nucleocapsid protein contributes to the NP-NP binding domain. Virology. 229:322-35.

Myers TM, Smallwood S, Moyer SA. 1999. Identification of nucleocapsid protein residues required for Sendai virus nucleocapsid formation and genome replication. J Gen Virol. 80:1383-91.

Nakamichi K, Saiki M, Sawada M, Takayama-Ito M, Yamamuro Y, Morimoto K, Kurane I. 2005. Rabies virus-induced activation of mitogen-activated protein kinase and NF-kappaB signaling pathways regulates expression of CXC and CC chemokine ligands in microglia. J Virol. 79(18):11801-12.

Niwa H, Yamamura K, Miyazaki J. 1991. Efficient selection for high-expression transfectants with a novel eukaryotic vector. Gene 108(2), 193-9.

Noe KH, Cenciarelli C, Moyer SA, Rota PA, Shin ML. 1999. Requirements for measles virus induction of RANTES chemokine in human astrocytoma-derived U373 cells. J Virol. 73(4):3117-24.

Noyce RS, Bondre DG, Ha MN, Lin LT, Sisson G, Tsao MS, Richardson CD. 2011. Tumor cell marker PVRL4 (nectin 4) is an epithelial cell receptor for measles virus. PLoS Pathog. 7(8):e1002240.

Noyce RS, Richardson CD. 2012. Nectin 4 is the epithelial cell receptor for measles virus.

Trends Microbiol. 20(9):429-39.

Osterhaus, A. D. M. E., J. Groen, F. G. C. M. Uytdehaag, I. K. G. Visser, M. W. G. van de Bildt, A. Bergman, and B. Klingeborn. 1989. Distemper virus in Baikal seals. Nature 338:209–210.

Pazdrak K, Olszewska-Pazdrak B, Liu T, Takizawa R, Brasier AR, Garofalo RP, Casola A. 2002. MAPK activation is involved in posttranscriptional regulation of RSV-induced RANTES gene expression. Am J Physiol Lung Cell Mol Physiol. 283(2):L364-72.

Plumet S, Duprex WP, Gerlier D. 2005. Dynamics of viral RNA synthesis during measles virus infection. J. Virol. 79(11):6900–6908

Plumet S, Gerlier D. 2005. Optimized SYBR green real-time PCR assay to quantify the absolute copy number of measles virus RNAs using gene specific primers. J Virol Methods 128:79-87.

Pratakpiriya W, Seki F, Otsuki N, Sakai K, Fukuhara H, Katamoto H, Hirai T, Maenaka K, Techangamsuwan S, Lan NT, Takeda M, Yamaguchi R.2012. Nectin4 is an epithelial cell receptor for canine distemper virus and involved in neurovirulence. J Virol. 86(18):10207-10.

Ramachandran A, Parisien JP, Horvath CM. 2008. STAT2 is a primary target for measles virus V protein-mediated alpha/beta interferon signaling inhibition. J. Virol. 82(17):8330–8338

Ray J, Fujinami RS. 1987. Characterization of in vitro transcription and transcriptional products of measles virus. J Virol. 61(11):3381-7.

Reymond N, Fabre S, Lecocq E, Adelaïde J, Dubreuil P, Lopez M. 2001. Nectin4/PRR4, a new afadin-associated member of the nectin family that trans-interacts with nectin1/PRR1 through V domain interaction. J Biol Chem. 276(46):43205-15.

Rima BK, Duprex WP. 2009. The measles virus replication cycle. Curr Top Microbiol Immunol. 329:77-102.

Robbins SJ, Bussell RH. 1979. Structural phosphoproteins associated with purified measles virions and cytoplasmic nucleocapsids. Intervirology 12:96-102.

Robbins SJ, Fenimore JA, Bussell RH. 1980. Structural phosphoproteins associated with measles virus nucleocapsids from persistently infected cells. J Gen Virol. 48:445-9.

Rockborn G. 1959. An attenuated strain of canine distemper virus in tissue culture. Nature. 184 (Suppl. 11), 822.

Roelke-Parker, M. E., L. Munson, C. Packer, R. Kock, S. Cleaveland, M. Carpenter, S. J. O'Brien, A. Pospischil, R. Hofmann-Lehmann, H. Lutz, G. L. M. Mwamengele, M. N. Mgasa, G. A. Machange, B. A. Summers, and M. J. G. Appel. 1996. A canine distemper virus epidemic in Serengeti lions (Panthera leo). Nature 379:441–445.

Saikia P, Gopinath M, Shaila MS. 2008. Phosphorylation status of the phosphoprotein P of rinderpest virus modulates transcription and replication of the genome. Arch. Virol. 153(4):615–626

Sato H, Honma R, Yoneda M, Miura R, Tsukiyama-Kohara K, Ikeda F, Seki T, Watanabe S, Kai C. 2008. Measles virus induces cell-type specific changes in gene expression. Virology. 375(2):321-30.

Sato H, Masuda M, Miura R, Yoneda M, Kai C. 2006. Morbillivirus nucleoprotein possesses a novel nuclear localization signal and a CRM1-independent nuclear export signal. Virology. 15; 352 (1): 121-30.

Schall TJ, Bacon K, Toy KJ, Goeddel DV. 1990. Selective attraction of monocytes and T lymphocytes of the memory phenotype by cytokine RANTES. Nature. 347(6294):669-71.

Schall TJ, Jongstra J, Dyer BJ, Jorgensen J, Clayberger C, Davis MM, Krensky AM. 1988. A human T cell-specific molecule is a member of a new gene family. J Immunol. 141(3):1018-25.

Schmid S, Mayer D, Schneider U, Schwemmle M. 2007. Functional characterization of the major and minor phosphorylation sites of the P protein of borna disease virus. J. Virol. 81(11):5497–5507

Schmid S, Metz P, Prat CM, Gonzalez-Dunia D, Schwemmle M. 2010. Protein kinase C-dependent phosphorylation of Borna disease virus P protein is required for efficient viral spread. Arch Virol. 155(5):789-93.

Schoehn G, Mavrakis M, Albertini A, Wade R, Hoenger A, Ruigrok RW. 2004. The 12 A structure of trypsin-treated measles virus N-RNA. J Mol Biol. 339(2):301-12.

Shaffer JA, Bellini WJ, Rota PA. 2003. The C protein of measles virus inhibits the type I interferon response. Virology. 315(2):389–397

Shanks GD, Lee SE, Howard A, Brundage JF. 2011. Extreme mortality after first introduction of measles virus to the polynesian island of Rotuma, 1911. Am J Epidemiol. 173(10):1211-22.

Spehner D, Kirn A, Drillien R. 1991. Assembly of nucleocapsidlike structures in animal cells infected with a vaccinia virus recombinant encoding the measles virus nucleoprotein. J Virol. 65:6296-300.

Sugai A, Kooriyama T, Sato H, Yoneda M, Kai C. 2009. Epitope mapping of canine distemper virus phosphoprotein by monoclonal antibodies. Microbiol. Immunol. 53(12):667–674

Sugai A, Sato H, Yoneda M, Kai C. 2012. Phosphorylation of measles virus phosphoprotein at S86 and/or S151 downregulates viral transcriptional activity. FEBS Lett. 586 (21): 3900-7.

Sugai A, Sato H, Yoneda M, Kai C. 2013. Phosphorylation of Measles Virus Nucleoprotein Affects Viral Growth by Changing Gene Expression and Genomic RNA Stability. J Virol. 87:11684-92.

Sugai A, Sato H, Hagiwara K, Kozuka-Hata H, Oyama M, Yoneda M, Kai C. 2014. Newly identified minor phosphorylation site threonine-279 of measles virus nucleoprotein is a prerequisite for nucleocapsid formation. J Virol. 88(2):1140-9.

Sun D, Luthra P, Li Z, He B. 2009. PLK1 down-regulates parainfluenza virus 5 gene expression. PLoS Pathog. 5(7):e1000525.

Tatsuo H, Ono N, Tanaka K, Yanagi Y. 2000. SLAM (CDw150) is a cellular receptor for measles virus. Nature. 406(6798):893-7.

Takahashi T, Arima Y, Kinoshita H, Kanou K, Saitoh T, Sunagawa T, Ito H, Kanayama A, Tabuchi A, Nakashima K, Yahata Y, Yamagishi T, Sugawara T, Ohkusa Y, Matsui T, Arai S, Satoh H, Tanaka-Taya K, Komase K, Takeda M, Oishi K. 2014. Ongoing increase in measles cases following importations, Japan, March 2014: times of challenge and opportunity. Western Pac Surveill Response J. 5(2):31-3.

Terao-Muto Y, Yoneda M, Seki T, Watanabe A, Tsukiyama-Kohara K, Fujita K, Kai C. 2008. Heparin-like glycosaminoglycans prevent the infection of measles virus in SLAM-negative cell lines. Antiviral Res. 80(3):370-6.

Thorne HV, Dermott E. 1977. Y-forms as possible intermediates in the replication of measles virus nucleocapsids. Nature. 268(5618):345-7.

Timani KA, Sun D, Sun M, Keim C, Lin Y, Schmitt PT. 2008. A single amino acid residue change in the P protein of parainfluenza virus 5 elevates viral gene expression. J. Virol. 82(18):9123–9133

Vincent S, Gerlier D, Manie SN. 2000. Measles virus assembly within membrane rafts. J Virol. 74(21):9911-5.

Warnes A, Fooks AR, Dowsett AB, Wilkinson GW, Stephenson JR. 1995. Expression of the measles virus nucleoprotein gene in Escherichia coli and assembly of nucleocapsid-like structures. Gene. 160:173-8.

Wechsler SL, Fields BN. 1978. Intracellular synthesis of measles virus-specified polypeptides. J Virol. 25(1):285-97.

Weston CR, Davis RJ. 2007. The JNK signal transduction pathway. Curr Opin Cell Biol. 19(2):142-9.

Wolfson LJ, Strebel PM, Gacic-Dobo M, Hoekstra EJ, McFarland JW, Hersh BS. 2007. Has the 2005 measles mortality reduction goal been achieved? A natural history modelling study. Lancet. 369(9557):191-200.

Wu X, Gong X, Foley HD, Schnell MJ, Fu ZF. 2002. Both viral transcription and replication are reduced when the rabies virus nucleoprotein is not phosphorylated. J Virol. 76(9):4153-61.

Yanagi Y, Takeda M, Ohno S, Hashiguchi T. 2009. Measles virus receptors. Curr Top Microbiol Immunol. 329:13-30.

Yang J, Koprowski H, Dietzschold B, Fu ZF. 1999. Phosphorylation of rabies virus nucleoprotein regulates viral RNA transcription and replication by modulating leader RNA encapsidation. J Virol. 73(2):1661-4.

Yoshikawa Y, Ochikubo F, Matsubara Y, Tsuruoka H, Ishii M, Shirota K, Nomura Y, Sugiyama M, Yamanouchi K. 1989. Natural infection with canine distemper virus in a Japanese monkey (Macaca fuscata). Vet Microbiol. 20(3):193-205.

ACKNOWLEDGEMENT

Without the guidance and expertise of my supervisor, Professor Chieko Kai (Laboratory Animal Research Center, Institute of Medical Science, The University of Tokyo, Tokyo), I would never have been able to finish my doctoral dissertation. First and foremost, I would like to express my very great appreciation to her for giving me the continued support, invaluable advice, and an opportunity to work towards a doctoral degree. I would also like to thank Associate Professor Misako Yoneda (Laboratory Animal Research Center, Institute of Medical Science, The University of Tokyo, Tokyo), my research supervisor, for her useful advice in radioisotope experiment that has helped me throughout my research. I would like to express my deep gratitude to Research Associate Hiroki Sato (Laboratory Animal Research Center, Institute of Medical Science, The University of Tokyo, Tokyo), my great mentor, for his patient guidance, gentle encouragement, excellent scientific and technical advice, and useful critiques of my research works. Special thanks should be given to all colleagues of Laboratory Animal Research Center for their kind cooperation.

Finally, I would like to express my sincere appreciation to my family for their support and encouragement. They always cheered me up and stood by me. My heartfelt thanks. These studies were supported by Grants-in-Aid from the Ministry of Education, Science, Sports, and Culture, Japan.

論文の内容の要旨

論文題目：Functional Analysis of Phosphorylation Modifications within Measles Virus Nucleoprotein and Phosphoprotein

（麻疹ウイルスＮ蛋白質及びＰ蛋白質におけるリン酸化修飾の機能解析）

氏名：菅井亮宏

麻疹ウイルスの構成蛋白質に対するリン酸化修飾の研究は、１９７０年代後半から始められており、N 蛋白質や P 蛋白質へのリン酸化修飾が報告されていた。しかしながら、それらのリン酸化修飾の機能についての詳細な報告はなく、ウイルス増殖におけるリン酸化修飾の意義は長らく不明なままであった。また、同じモービリウイルス属に分類されるイヌジステンパーウイルスや牛疫ウイルス等の、動物に感染するウイルスおいても、構成蛋白質のリン酸化とその影響については十分に解明されていない。そのため、筆者は、比較的解析が進んでいる麻疹ウイルスを用いて、N 蛋白質及び P 蛋白質のリン酸化修飾の役割を明らかにするため、詳細な機能解析を行った。モービリウイルス属のウイルスは、互いに多くの類似した性質を持つことから、本研究で得られた知見は、麻疹ウイルスのみならず、イヌジステンパーウイルスや牛疫ウイルス等の獣医学的に重要なウイルスにおけるリン酸化修飾について考える上でも有用であると考えられる。

CHAPTER1

P 蛋白質リン酸化のウイルス RNA 合成への影響の解析

麻疹ウイルス P 蛋白質はウイルスゲノムの転写及び複製に不可欠な因子であり、N 蛋白質と共にウイルス RNA ゲノムに結合し、ヌクレオカプシドを形成する。N 蛋白質及び P 蛋白質はリン酸化修飾を受けることが知られており、幾つかのウイルスで P 蛋白質のリン酸化

修飾がウイルスゲノムの転写及び複製効率に影響を及ぼすことが報告されてきたが、麻疹ウイルスの P 蛋白質に関する報告はなかった。一方で、近年、当研究室では N 蛋白質のリン酸化修飾が、ウイルスゲノムの転写及び複製の効率に影響を与えることを報告した。そこで、本研究では、N 蛋白質及び P 蛋白質のリン酸化修飾とウイルスゲノムの転写複製効率の関連性について解析した。

ウイルスゲノムの転写複製と N 及び P 蛋白質のリン酸化状態との関連性を調べるため、N 蛋白質のリン酸化部位変異体（S479A、S510A、S479A/S510A）と P 蛋白質を、L 蛋白質及びミニゲノム RNA と共に培養細胞内で共発現し ^{32}P 標識して、N 及び P 蛋白質のリン酸化状態を解析した。また、ミニゲノムレポーターアッセイにより転写複製活性を測定し、N 及び P 蛋白質のリン酸化状態との関連性を調べた。P 蛋白質のリン酸化部位変異体（S86A/S151A、T49A/S86A/S151A）を用い、N 及び P 蛋白質のリン酸化状態を解析し、転写複製活性への影響を評価した。また、転写と複製のどちらが影響を受けるのか調べるため、定量 PCR によりミニゲノム RNA の転写複製産物の量を測定した。

これらの解析の結果、N-P 蛋白質間相互作用により、N 蛋白質のリン酸化状態の変化が、P 蛋白質のリン酸化状態に影響を与えることが示唆された。この N 蛋白質のリン酸化状態の変化によって影響を受ける部位は、P 蛋白質の８６及び１５１番目のセリン残基であり、これらの部位へのリン酸化がウイルス RNA 合成を著しく阻害することが明らかとなった。また、N 蛋白質リン酸化率とウイルスゲノムの転写及び複製効率に相関性は見られなかったが、P 蛋白質リン酸化率がウイルス RNA 転写及び複製量と逆相関することが示された。定量 PCR の結果から、S86 及び S151 のリン酸化は、ウイルス RNA の転写を選択的に抑制することが示唆された。

以上の結果から、N 蛋白質のリン酸化状態はウイルスゲノムの転写及び複製効率に直接的にではなく、P 蛋白質のリン酸化状態を変化させることにより間接的に作用するものと考えられた。P 蛋白質の S86 及び S151 のリン酸化状態が高いほど転写及び複製効率が低下するという逆相関関係が見られ、S86 及び S151 へのリン酸化は P 蛋白質の活性には必要とされないが、これらのサイトへのリン酸化がウイルス RNA 転写の下方調節に働く可能性が示唆された。

CHAPTER2

組換え麻疹ウイルスによる N 蛋白質リン酸化の機能解析

麻疹ウイルスにおける N 蛋白質の主要な役割の一つは、ウイルスＲＮＡゲノムを物理的に被覆し保護することである。近年、当研究室では、N 蛋白質のリン酸化部位の解析を行い、主要な２箇所のリン酸化部位を同定し、このリン酸化修飾がミニゲノム系においてウイルスゲノムの転写及び複製の効率に影響を与えることを報告した。しかしながら、それらのリン酸化修飾が実際のウイルス増殖に与える影響は不明であった。今回、筆者はリバースジェネティクス法によって N 蛋白質のリン酸化部位を変異させた組換えウイルスを作出し、リン酸化修飾がウイルスの増殖効率等に与える影響を解析した。

各リン酸化部位に変異を導入した組換えウイルスの力価を測定し、増殖曲線を作製した。同時に、各組換えウイルスの遺伝子発現活性を比較する為、感染細胞内の N 蛋白質量を経時的に測定した。続いて、パルスチェイスアッセイ及びヌクレアーゼ耐性試験により、N 蛋白質のリン酸化状態とウイルスゲノムの安定性の関連を評価した。

各組換えウイルスの解析により、増殖初期には野生型に比べ変異ウイルスの遺伝子発現及び増殖が上昇することが明らかとなった。また、このウイルス増殖の上昇に伴い、著しいサイトカインの誘導が見られた。一方、増殖がプラトーに達すると N 蛋白質のリン酸化状態が低いほど増殖が高いという逆相関関係が見られた。また、N 蛋白質のリン酸化率が低いほどウイルスゲノムのヌクレアーゼ耐性が増強し、安定化することが明らかとなった。

増殖初期において、リン酸化部位変異ウイルスでN遺伝子発現上昇が見られたことから、リン酸化が何らかの機構でウイルス遺伝子の発現調節に関わる可能性が示唆された。また、増殖後期における N 蛋白質のリン酸化レベルとウイルス増殖の逆相関は、リン酸基とウイルスゲノムの電荷的反発によるゲノムの不安定化を介したものであることが推察された。更に、P 蛋白質が N 蛋白質に結合することで、N 蛋白質のリン酸化状態の低下を引き起こし、このことがヌクレオカプシド形成の効率化に寄与していることが示唆された。

CHAPTER3

新しく同定された N 蛋白質のリン酸化部位とその役割

麻疹ウイルスのＮ蛋白質はウイルスゲノムRNAに結合してヌクレオカプシドを形成し、これが足場となってウイルスゲノムの転写及び複製が行われる。これまで筆者は、N 蛋白

質の主要な二カ所のリン酸化部位について、ウイルス増殖における役割を解析してきたが、これら二カ所以外にもリン酸化部位の存在が示唆されていた。本研究では、筆者は N 蛋白質の新たなリン酸化部位を同定し、その役割を明らかにするため、機能解析を行った。

MS 解析（質量分析法）により推定リン酸化部位を絞り込み、アラニンスキャン及び ^{32}P ラベルによってリン酸化部位を同定した。リン酸化部位を変異させた N 蛋白質を作製し、ミニゲノムアッセイによりウイルスの転写及び複製への影響を評価した。更に、P 蛋白質との相互作用への影響を共沈実験により確認した。また、電子顕微鏡による解析、密度勾配遠心法、脱リン酸化酵素を用いた解析により、リン酸化とヌクレオカプシド形成の関連性を検索した。

MS 解析の結果、リン酸化部位の候補が九カ所見つかり、アラニン置換変異体を用いた解析で、279 番目のスレオニン残基がリン酸化されていることが明らかとなった。このリン酸化部位を変異させると、N 蛋白質と P 蛋白質の相互作用には影響しなかったが、ミニゲノムアッセイにおいて転写及び複製の活性が著しく損なわれた。更に、電子顕微鏡を用いた解析において、このスレオニン残基のアラニン置換変異体はヌクレオカプシドを形成できず、異常な構造体が観察された。また、このリン酸化部位の脱リン酸化処理によって、ヌクレオカプシドの構造が不安定化することが示唆された。

N 蛋白質 279 番目のスレオニン残基のリン酸化修飾は、正常なヌクレオカプシド構造の形成に不可欠であることが明らかとなった。このリン酸化修飾は、ウイルスゲノムの転写及び複製に必須であり、ウイルスが増殖する上で非常に重要な役割を担っていると考えられる。

結び

本研究において、筆者は N 蛋白質及び P 蛋白質のリン酸化修飾が、それぞれの機能に及ぼす影響について、リン酸化部位変異体や組換えウイルスを用いることで詳細に解析してきた。その結果、P 蛋白質のリン酸化はウイルス RNA の転写制御に関与することが示唆され、N 蛋白質のリン酸化はウイルス構成蛋白質の発現量、ウイルスゲノム RNA の安定性に影響を及ぼすことが示された。また、新規に同定された N 蛋白質の N 末端側のリン酸化修飾は、ヌクレオカプシドの形成に必須であることが明らかとなった。本研究は、麻疹ウイルス構成蛋白質に対するリン酸化修飾の機能について、組換えウイルスを用いて詳細に解析を行った初めての報告であり、リン酸化修飾が持つ生物学的意義について考察する上で重要な多くの新しい知見が示された。ここで得られた知見は、麻疹ウイルスに限らず、近縁のイヌジステンパーウイルスや牛疫ウイルスといった獣医学領域で重要なウイルスを含め、広くパラミクソウイルス全般に有用な知見を与えると考えられる。